Heat Transfer Characteristics of Conventional Fluids and Nanofluids in Micro-Channels with Vortex Generators: A Review

Mushtaq T. Al-Asadi [1,2,*], **Hussein A. Mohammed** [3,*] and **Mark C. T. Wilson** [2]

[1] Business Development Department, Basra Oil Company, Ministry of Oil, Basra 240, Iraq
[2] Institute of Thermofluids, School of Mechanical Engineering, University of Leeds, Leeds LS2 9JT, UK; m.wilson@leeds.ac.uk
[3] WA School of Mines-Minerals, Energy & Chemical Engineering, Curtin University, Perth, WA 6102, Australia
[*] Correspondence: mushtaq@boc.oil.gov.iq or dr.eng.mushtaq@gmail.com (M.T.A.-A.); hussein.mohammed@curtin.edu.au or hussein.dash@yahoo.com (H.A.M.)

Abstract: An effective way to enhance the heat transfer in mini and micro electronic devices is to use different shapes of micro-channels containing vortex generators (VGs). This attracts researchers due to the reduced volume of the electronic micro-chips and increase in the heat generated from the devices. Another way to enhance the heat transfer is using nanofluids, which are considered to have great potential for heat transfer enhancement and are highly suited to application in practical heat transfer processes. Recently, several important studies have been carried out to understand and explain the causes of the enhancement or control of heat transfer using nanofluids. The main aim upon which the present work is based is to give a comprehensive review on the research progress on the heat transfer and fluid flow characteristics of nanofluids for both single- and two- phase models in different types of micro-channels. Both experimental and numerical studies have been reviewed for traditional and nanofluids in different types and shapes of micro-channels with vortex generators. It was found that the optimization of heat transfer enhancement should consider the pumping power reduction when evaluating the improvement of heat transfer.

Keywords: heat transfer; nanofluids advantages and disadvantages; thermal hydraulic performance; vortex generators; micro-channel

1. Introduction

Since 1931, researchers have explored ways to manage the heat flux generated from electrical devices and offer better heat transfer rates using different approaches to enhance the heat transfer in mini and micro cooling systems [1].

Nowadays, the impact of heat transfer and fluid flow have become more interesting and challenging simultaneously due to rapid developments in electronic and electrical devices and systems which become increasingly small in size, light in weight but high in heat transfer dissipation demands. Therefore, enhancing the heat transfer in such systems has been a strong motivation for this current research [2].

A possible and most effective approaches to enhance the heat transfer is the design of a heat sink; the most popular heat sink used in air-cooled systems is a plate-fin heat sink (PFHS) because of its simplicity to manufacture. Many investigations of PFHSs have studied and optimized the fins' height, thickness, and separation, yielding predictions of heat transfer and entropy [3–6]. Other designs such as pinned heat sinks (PHSs) have also been considered in both inline and staggered arrangements to enhance the heat transfer rate [7]. They can take several shapes such as rectangular, square, circular, elliptical, NACA and drop form [1,8–11]. The key components in the cooling of computer systems, and many other applications such as air conditioning are heat exchangers and heat sinks [12–15].

Based on the working fluid, heat exchangers are generally classified as gas, liquid, or a combination. Some examples of heat exchangers are shown in Figure 1. Many studies have shown that the liquid heat exchangers and heat sinks systems had great potential for enhancing the heat transfer compared to gas systems based on some of their thermal properties, which is higher in the liquid than in the gas [16,17].
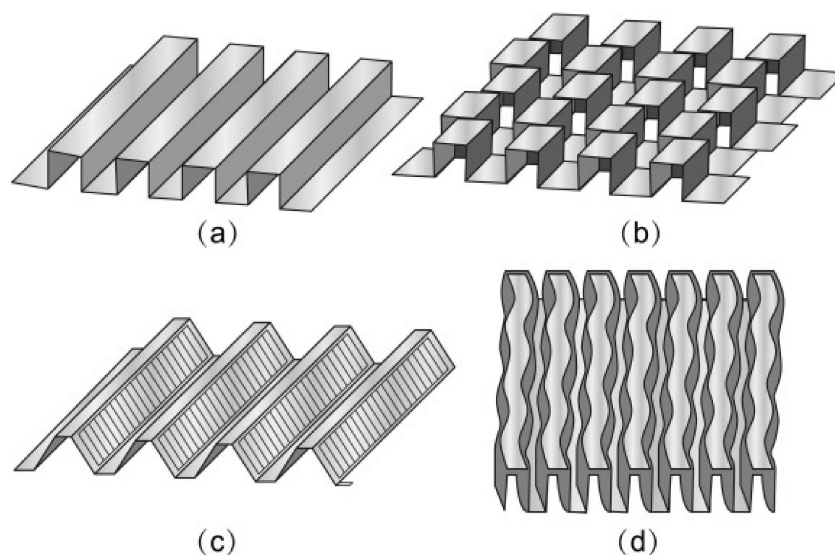

Figure 1. Heat exchanger classification (**a**) plain rectangular fins: (**b**) offset strip fins, (**c**) louvered fins (**d**) wavy fins.

Continuing developments in electronic and electrical devices and the increased heat density associated with miniaturization mean that the thermal management of high heat fluxes remains an active area of research [18].

However, another approach to improve the heat performance of the cooling systems is to improve the thermo-physical properties of the coolants—for example, by developing nanofluids [14,19–21], which have used widely in industry and studied extensively for their impact on the environment [22–24]. Alternatively, the geometry of the heat sinks can be adapted to improve heat transfer—for example, by modifying the pins in PHSs or the channels in PFHSs. One very successful approach for air applications is the use of micro-channels. Note that the micro-channels first appeared in 1981 [25].

Many ways by which the heat transfer might be enhanced, such as suggestions of new designs of the geometry and/or advanced fluids, can be used [26]. Various geometries have been designed to achieve a high performance of heat transfer using an extended surface area [27,28].

Many experimental and numerical studies have investigated the heat transfer and fluid flow performance of various modified geometries such as micro-channels with grooves and ribs [29–32]. The effect of vortex generators (VGs) on heat transfer and fluid flow characteristics were investigated experimentally in 1969 [33].

In addition to the surface area enhancement, vortex generators can be considered as a geometry improvement, which creates secondary flows that can enhance the heat transfer [34,35].

In the revolution of advanced manufacturing processes, VGs can take up various forms such as protrusions, wings, inclined blocks, winglets, fins, and ribs [2,36], and have been used to enhance heat transfer in different geometries such as circular and non-circular ducts under turbulent flow [34,37,38]. They have also been used in laminar flow, with flat plate-fins in rectangular channels [37–39], tube heat exchangers [40], heat sinks [41,42], and rectangular narrow channels [43,44], as shown in Figure 1.

One of the promising systems by which high-performance heat rejection can be achieved is micro- and mini-scale systems, such as micro-channel heat exchangers and

heat sinks [12,15,45–47]. They are different from traditional channels and can be classified according to their associated hydraulic diameters, D_h, [48–50]. The classification of the channel according to Mehendale et al. [49] is that the conventional channels with $D_h > 6$ mm, compact Passages 1 mm$< D_h \leq 6$ mm, meso-channels 100 mm$< D_h \leq 1$ mm, and micro-channels 1 μm $< D_h \leq 100$ μm. while Kandlikar and Grande [50] had another classification of the channel, the that the conventional channels with $D_h > 3$ mm, mini channel 1 mm$< D_h \leq 3$ mm, micro-channels 10 μm $< D_h \leq 200$ μm, transitional channels 0.1 mm$< D_h \leq 10$ mm, and the Molecular nanochannels with the $D_h \leq 0.1$ μm.

On the other hand, using advanced fluids instead of traditional fluids (e.g., air and water) has become common and effective. It can be a combination of two fluids like mixing water and glycerin [51], or it can be a suspension of particles in a liquid, which is well known as a nanofluid [52]. Recently, the use of nanofluids has been applied to manage the heat transfer in batteries [53–56].

In this article, a comprehensive review has been conducted to focus on heat transfer performance with different modifications of both the fluid and geometry. Furthermore, the influence of evaluating heat transfer enhancement together with the pressure penalty resulted from the modifications of the geometry and the fluid. This review paper is divided into three main sections that consider straight micro-channels, vortex generators, and nanofluids.

2. Uniform Micro-Channels

This section provides an idea of the investigations that have been carried out on a uniform channel. It is divided into two sections: single-phase flow and two-phase flow.

2.1. Single Phase Flow

A numerical investigation of various shapes of rectangular micro-channels with the range of width 44–56 μm, height 287–320 μm, and length 10 mm was conducted by Shkarah et al. [57]. The materials used were aluminum, silicon, and graphene. Different values of volumetric flow rate and heat flux with fully developed laminar flow of water were utilized. The results showed that the thermal resistance was reduced by using graphene in the micro-channel. However, the findings have not yet been confirmed experimentally and the numerical method considered the thermo-physical properties of the materials as non-temperature-dependent, which may affect the results when compared to the experimental setup.

Laminar flow of deionized water in a copper rectangular micro-channel with a hydraulic diameter ranging from 200 to 364 μm and with a length of 120 mm was numerically studied by Lee et al. [58]. The finite volume method was implemented to determine the Nusselt number at various aspect ratios. The study presented the distribution of local and average Nusselt numbers as a function of non-dimensional axial distance. The researchers proposed correlations which helped to enhance the heat transfer. The proposed correlations considered the entrance length effect on heat transfer rate and were in very good agreement with previous experimental studies. It was found that the new correlation was applicable for thermally developed flow for local and average Nusselt number under laminar flow.

Mansoor et al. [59] performed three-dimensional simulations of a rectangular micro-channel using single-phase laminar flow (Re ranged from 500 to 2000) of deionized water as a working fluid. A heat flux of 130 W/cm^2 was considered to investigate the thermal characteristics in a copper micro-channel. The study used FLUENT commercial software, (New York, NY, USA) and the results were compared with previous numerical and experimental works, showing good agreement. It was found that the heat transfer coefficient was decreased as the heat flux increased. In addition, a high Reynolds number and heat flux led to a transition from single- to two-phase flow, while there was no transition when the heat flux was less than 100 W/cm^2.

An experimental study of a copper rectangular micro-channel with a hydraulic diameter in the range of 318–903 μm and length of 24.5 mm was conducted by Lee et al. [60], using

deionized water as a working fluid. The study used laminar and turbulent flows, with the Reynolds number ranging from 300 to 3500 to investigate the heat transfer and fluid flow regimes using single-phase flow. The results showed that heat transfer was increased as the channel size decreased. However, decreasing the dimensions of the rectangular channel requires more pumping power resulting from an increase in the associated pressure drop.

Deng et al. [61] compared a traditional rectangular cross-section copper micro-channel with an omega shape micro-channel heat sinks of the same hydraulic diameter with ethanol and deionized water as two-phase boiling flow, as shown in Figure 2. The results showed that water is better than ethanol in both micro-channel types. Moreover, using the omega micro-channel decreased the pressure drop compared to the conventional rectangular micro-channel.
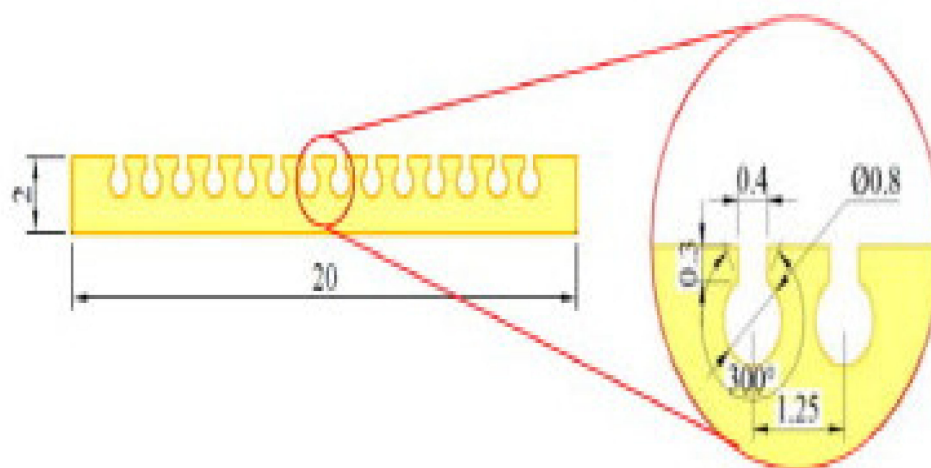

Figure 2. Micro-channel omega shape in mm [61] © Elsevier, 2015.

Micro-channels can be used not only with liquid but also with gas as a working fluid; Balaj et al. [62] studied the influence of shear stress in micro- and nano-channels using constant wall heat flux. The simulation model used the direct-simulation Monte Carlo method. It was found that there is a sensible effect of the magnitude of viscous dissipation on heat and flow performance; therefore, it should be considered in heat transfer predictions. The study also showed that the heat transfer is significantly enhanced when the heating condition is applied, while the heat transfer is decreased while utilizing the cooling condition.

Xia et al. [63] numerically studied the heat transfer and fluid flow characteristics of a liquid-cooled heat sink with three different inlet and outlet locations named c, I, and z, and different header shapes that feed the micro-channels, as shown in Figure 3. The traditional shape of a rectangular micro-channel was compared with a triangular shape. The results showed that the best geometry is rectangular and the best location of the inflow regime was I, then c, then z. Additionally, the results showed that better heat transfer characteristics were achieved with the rectangular header shape. However, the results showed that using the position shown in Figure 3c was the best design when using a volume flow rate of 150 mL/min. This can be attributed to the velocity uniformity compared to the trapezoidal and triangular shapes.

Heat transfer can be enhanced by applying a magnetic field on water-based Fe_3O_4, as indicated by the study by Ghasemian et al. [64]. They investigated the heat transfer characteristics of a rectangular channel with a width of 0.2 cm and length of 2 cm subjected to constant and variable magnetic fields under laminar flow. The finite volume method was used to solve the governing equations and two-phase mixture flow was implemented in the study. The results showed that three parameters enhanced the heat transfer, namely frequency and locations (a, b) of magnetic fields, as shown in Figure 4. Noticeable enhancement of heat transfer appeared at fully developed flow, especially when applying the magnetic field. Moreover, it was found that using an alternating magnetic field was better

than a constant one by approximately 1.6 times. Using an alternating magnetic field acts as a vortex generator to frequently disturb the fluid.
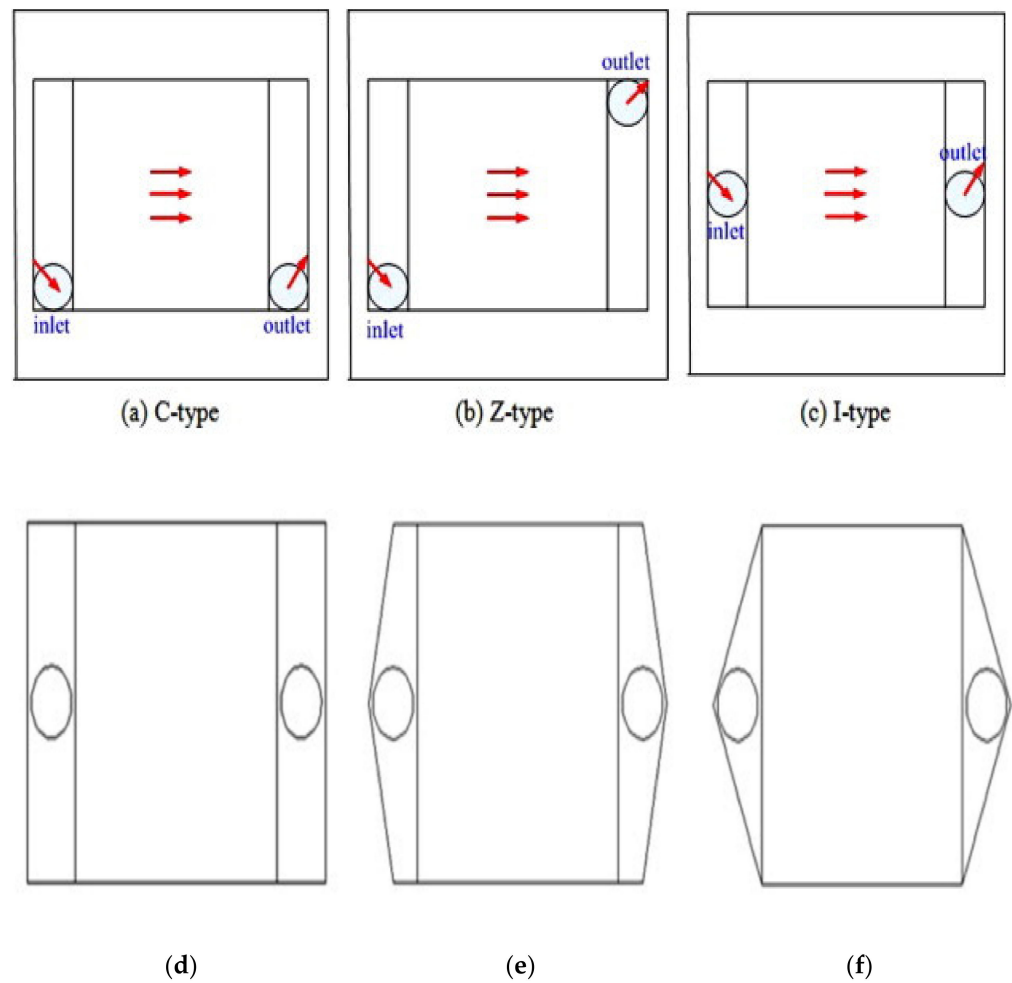
Figure 3. Different inlet and outlet positions and header shapes of micro-channel heat sinks [63] © Elsevier, 2015. (**a**) C-type; (**b**) Z-type; (**c**) I-type; (**d**) rectangular; (**e**) trapezoidal; (**f**) triangular.

Figure 4. Magnetic field distribution to enhance the heat transfer [64] © Elsevier, 2015.

A review of numerical and experimental investigations focusing on the heat transfer and air-side flow using a fin and tube heat exchanger was presented by Pongsoi et al. [65].

The study summarizes a significant effect such as tube arrangement, operating conditions, and fin configurations. More than 35 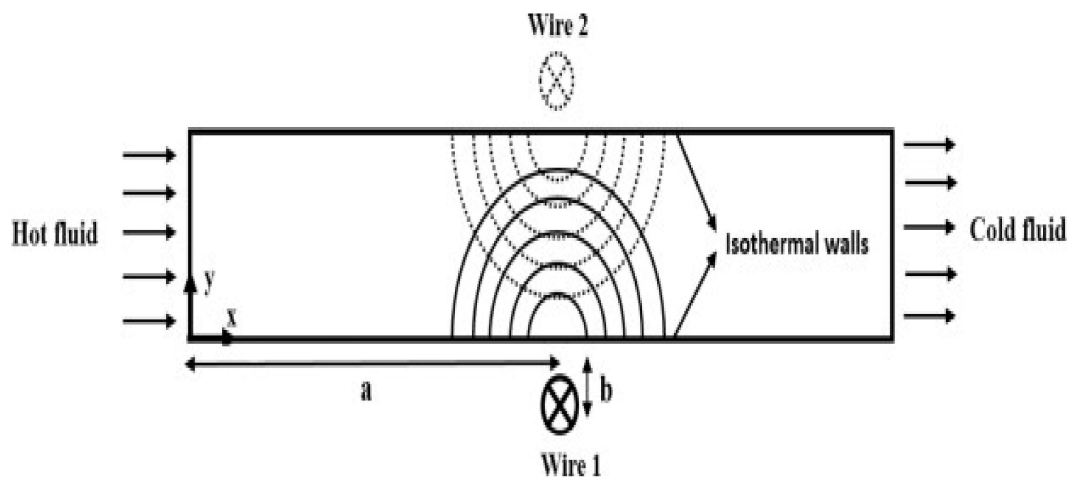articles related to heat exchangers were considered, representing the experimental studies from the very early period. The study used geometry design by comparing circular and spiral fins. It concluded that 57% of the heat exchangers used a spiral fin; thus, the recommendation of the investigation was to use a spiral fin instead of a circular fin in heat exchangers. Moreover, Pan et al. [66] presented the effect of different inlet distribution manifold for different widths of rectangular micro-channels. The investigation considered different dimensions of the inlet design of a Z-shape to examine the effect of inlet distribution and the width of the channel on optimal design of a micro-channel. The results showed that the width of the channel had a significant influence on the optimization results.

Another review of micro- and mini-channel geometries is that of Dixit and Ghosh [48]. The study illustrated previous work in a single-phase flow with heat exchangers and heat sinks in various types of flow such as laminar, turbulent, developing flows, and fully developed flow. It also presented the heat transfer performance such as convective heat transfer under the condition of constant wall temperature and constant heat flux. The application and fabrication of micro- and nano-scales were also adopted in this investigation. It was concluded that it is still difficult to produce channels of micro-size due to manufacturing limitations; however, micro-channels can be produced as parts, but it is still not easy to combine the parts to produce micro-channels. Many issues can be found when producing micro-channels from parts such as the accuracy of having equal distance between channels. Moreover, the reliability of the glue for a specific application, the conductivity of the glue used to combine the parts, and avoiding having a layer of the glue might influence the heat transfer performance.

A numerical and experimental investigation of heat transfer and fluid flow performances in a bronze rectangular micro-channel with dimensions of 1 and 0.3 mm was presented by Gamrat et al. [67]. Water as a working fluid with a Reynolds number in the range of 200–3000 was considered to investigate the mixed convective heat transfer performance. The results of the numerical study showed that there was no sensible influence on the Nusselt number when the channel dimension changed from 1 to 0.1 mm. Due to the limitation of the experimental measurement, the impact of this change has not been measured.

Laminar flow in different rectangular copper micro-channels with a width and height 231 μm and 713 μm, respectively, was studied experimentally and numerically by Qu and Mudawar [68]. Deionized water at a Reynolds number in the range of 139–1672 was considered as the working fluid. Two heat flux values (100 and 200 W/cm^2) were applied on the bottom wall to investigate the fluid flow and heat transfer performance. It was found that the outlet temperature of the fluid decreased at a high Reynolds number while the pressure drop increased. It was also found that there was not much difference in temperature at the top wall of the micro-channels; therefore, it can be considered as an adiabatic wall.

However, most recent numerical studies considered the top wall (the wall which is opposite the wall where heat flux was applied to) as an adiabatic wall. This is because the low heat transfer at the top wall might transfer from the walls by conduction and the fluid by convection, especially when using a plastic top wall.

2.2. Two-Phase Flow

A considerable number of studies have been carried out on the design of micro-channels using two-phase models, as can be seen in the following paragraphs.

An experimental investigation of the heat transfer performance was conducted by Hsu et al. [69] using different orientations of copper rectangular micro-channels with a hydraulic diameter of 440 μm, heat flux of 25 kW/m^2, and mass flux of 100 and 200 kg/m^{2}s. Two-phase boiling flow and HFE-7100 as a working fluid was considered. The setup investigated the effect of the inclination from the horizontal to the vertical position on

boiling heat transfer. It was found that the heat transfer coefficient rose with the vapor quality and peaked when it reached 0.6 for the upward position.

Suwankamnerd and Wongwises [70] studied two-phase air–water flows in a copper rectangular micro-channel having 267 μm hydraulic diameter with low Reynolds number. The setup used a separate flow model as well as a homogeneous flow model to estimate the pressure drop using the Friedrel correlation, which is used to measure the pressure drop in two-phase flow. The investigation showed enhancement in the Nusselt number of 120% compared to single-phase flow.

In addition, Mirmanto [71] studied the heat transfer coefficient in various dimensions of a single copper rectangular micro-channel with a horizontal position. Boiling deionized water at 98 °C at the inlet as a working fluid, 125 kPa as inlet pressure, 800 kg/m^2 of mass flux, and various values of heat flux were used in this study. The results showed that there was good agreement between the experimental measurements and the numerical simulation, especially in the pressure gradient. It was effective at the low pressure generated. At fixed heat and mass flux, it was found that the heat transfer coefficient went down with the quality in the smallest hydraulic diameter, while it was increased significantly with the other diameters.

Konishi et al. [72] studied the effect of boiling flow on flow and heat transfer maps. The geometry was a copper rectangular channel consisting of two heating walls fixed opposite each other with liquid and mass inlet velocities ranging from 0.1 to 1.9 m/s and 224.2 to 3347.5 kg/m^2 s, respectively; and a temperature of inlet sub-cooling in the range of 2.8–8.1 °C. Heat transfer and fluid flow measurements were adopted to examine the flow performance. It was found that the temperature distribution improved as the gravity rose, while it decreased in micro-gravity.

Gan et al. [73] experimentally investigated the pressure drop characteristics of two-phase flow in a triangular silicon micro-channel with dimensions of 300, 212, and 155.4 μm in width, depth, and hydraulic diameter, respectively. Acetone was considered as a working fluid under various ranges of inlet temperature and pressure, mass velocity, superheat, outlet quality, and heat flux. The pressure drop and boiling flow were performed. The outcome of the study was a new correlation which considered the functionality of mass flux and, therefore, the error of predicting the acetone data with 12.56% of mean absolute error.

Fang et al. [74] proposed a correlation of flow boiling to investigate the heat transfer regime using a copper rectangular tube. The study adopted H$_2$O, R718 as a working fluid, two-phase laminar and turbulent flows. More than 1050 data points of water boiling flow for mini- and micro-channels were collected. The results showed that the proposed correlation was applicable to many refrigerant fluids, especially for R410 and NH3.

Shojaeian and Koşar [75] reviewed previous experimental studies on micro- and nano-geometries using boiling flow. These geometries were in various shapes such as rectangular, triangular, and cylindrical cross-section. Heat transfer and fluid flow characteristics were presented and compared with different parameters such as single-phase and two-phase flows. It was found that the nano- and micro-structures enhanced the heat transfer rate of systems. Furthermore, the manufacturing ability increased to produce such complex shapes of nano-/micro-channels. Consequently, manufacturing nano-/micro-configurations had some finishing issues related to the surface. This can be tackled by coating the surface.

Asadi et al. [76] reviewed the validity of experimental correlations on pressure-drop and heat-transfer characteristics in single- and two-phase flows with different geometries of micro-channel. The investigation used 219 papers of experimental and numerical studies (from 1982 to 2013). It was found that, before 2003, the researchers focused on experimental and analytical investigations, while after 2003, the focus turned to numerical studies. It also indicated that approximately 76% of researchers considered the laminar flow using single-phase flow. This is because the behavior of the laminar flow can be predicted and agreed with the experimental data. However, an important factor has not been considered in this study, which is the energy consumption of using turbulent flow. For example,

using turbulent flow will cost more pumping power to derive the flow, resulting in more energy consumption.

In summary, straight micro-channels represented the starting stage in converting from using conventional channels to micro-sized channels in various applications of micro-electrical and micro-electronical chips. As reviewed in the previous sections, micro-channels have rapidly received high attention by many researchers in different investigations, both numerical and experimental, as presented in Figure 5.
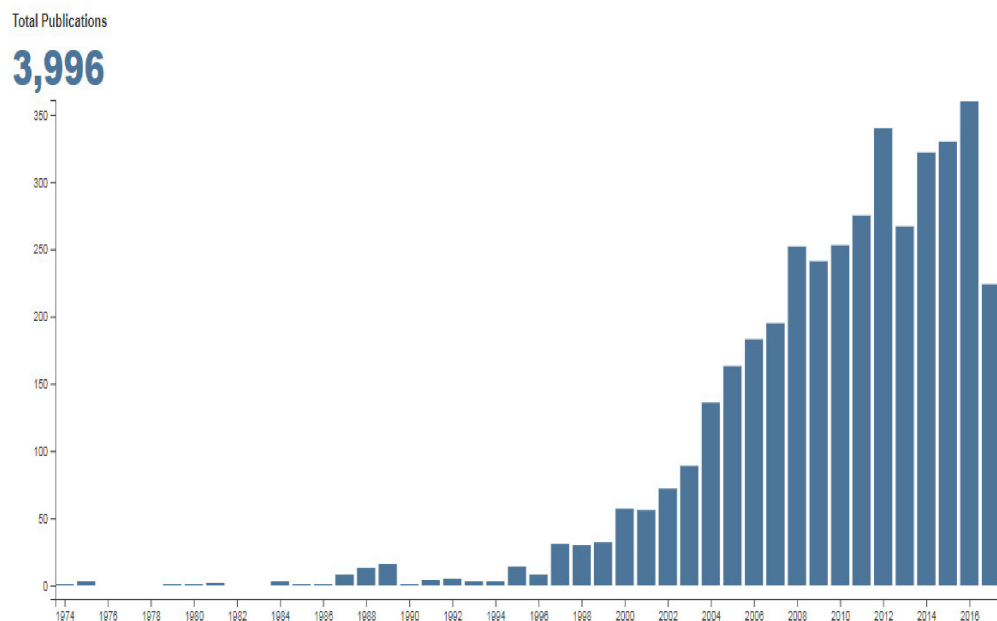

Figure 5. Growth in number of publications of micro-channels [77] © Elsevier, 2017.

The limitation in manufacturing micro-channels was a reason for a reduction in experimental studies. Another reason is the high price incurred to manufacture micro-channels. It is to be expected that in the near future, the manufacturing developments will easily allow production of micro-sized channels. Therefore, there is a real need to develop straight micro-channels into channels with complex shapes such as zigzag, wavy, and curved micro-channels to enhance the heat transfer. In addition, increasing the surface area and developing the secondary flow in the micro-channels also contributes to enhance the heat transfer rate. This can be achieved by adding some objects to increase the surface area and disturb the flow to develop the secondary flow.

2.3. Curved and Tapered Rectangular Micro-Channels

Research on curved micro-channels has also received recent attention by many researchers because of the high thermal and flow performance produced by these geometries, as elaborated in the following paragraphs.

Numerical simulation of laminar flow using water as a cooling fluid was performed by Guo et al. [78]. They investigated the influence on heat transfer performance of a curved micro-channel with a square cross-section, as presented in Figure 6. This micro-channel had a width and curve radius of 0.2 mm and 30 mm, respectively, and a Reynolds number in the range of 100–865. It was found that at high convection heat transfer, the synergy principle method can be applied. Note that this method applied to increase the accuracy of the solution because it considers the heat transfer at the outer wall. This method is applicable for such a curved channel because it presents the heat transfer accurately for the outer walls with consideration of the fluid flow.
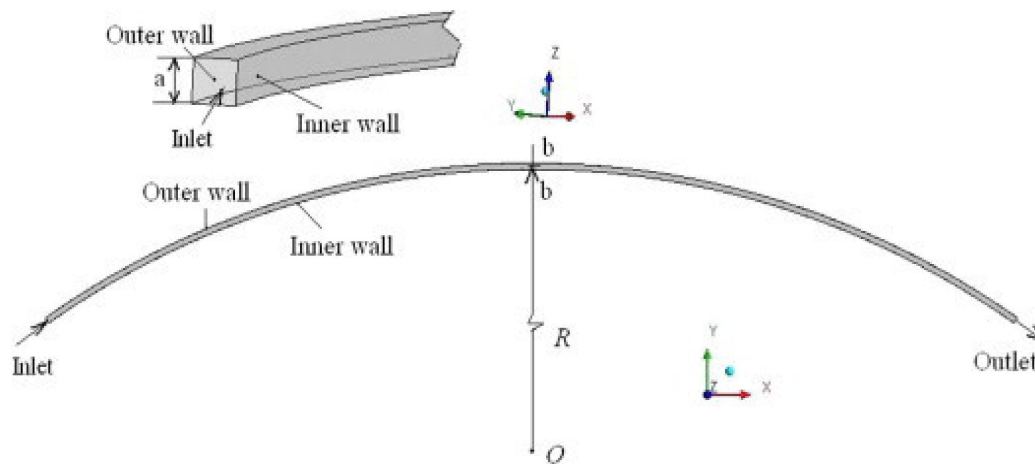
Figure 6. Curved duct with square cross-sectional area [78] © Elsevier, 2011.

Chu et al. [79] performed both experimental and numerical investigations of curved rectangular micro-channels with different diameters to study the influence of different diameters of the curve on flow characteristics. The Reynolds number was in the range of 80–876 and deionized water as a working fluid was considered. The results showed good agreement between the simulation and experiments. It was found that the curvature of the channel geometry increased the velocity at the outer wall, thus leading to enhancement of the heat transfer performance but increasing the friction factor.

A numerical study of a tapered aluminum micro-channel by Dehghan et al. [80] investigated the influence of different tapering geometries on pressure drop reduction using laminar flow and a constant heat flux of 100 W/cm^2. The width of the channel was fixed at the inlet to be 200 μm, while the outlet width was in the range of 75 to 200 μm with the channel length being 12,000 μm. It was found that the Poiseuille number and Nusselt number rose with tapering. The optimum heat transfer characteristics were found at an outlet-to-inlet width ratio of 0.5. However, with no consideration of the pressure drop in this study, it might be worth considering the pressure drop effect using the channel inlet, which can be taken in a range from 75 to 200 μm.

## 3. Non-Uniform Channels and Vortex Generators

The effect of vortex generators (VGs) on the heat transfer and fluid flow characteristics were investigated experimentally in 1969 [33]. Two types of vortex generators were classified based on the direction of the axis of rotation of the vortices generated.

Several parameters such as the geometry, shape, and position of the VGs might play a crucial role in enhancing the heat transfer, and the VG shape can be classified into rectangular, delta wings, and winglets, as presented earlier in [81]. However, the wing and winglet VGs are only suitable for air-based heat sinks. Various investigations have also indicated potential benefits of using VGs with laminar flow at different Reynolds numbers [35,43,82].

3.1. Non-Uniform Channels

Many experimental and numerical investigations have considered geometrical modifications of uniform channels to enhance the heat transfer performance. Liu et al. [83] conducted an investigation of the influence of geometry on heat and flow maps using turbulent air flow in a modified square channel with cylindrical slots of various diameters, as shown in Figure 7a. The finite volume method was used to solve the governing equations, utilizing FLUENT 12.1. The results emphasized that using cylindrical grooves and square ribs in the channel (see Figure 7b) enhanced the heat transfer characteristics compared to the uniform channel due to the extended surface area and the generation of vortices by disturbing the flow. However, the pressure drop of the square-ribbed channel was higher

than the cylindrical grooves channel and the uniform channel. This study agreed with the results of cylindrical grooves in mini channels performed by Tang et al. [84].
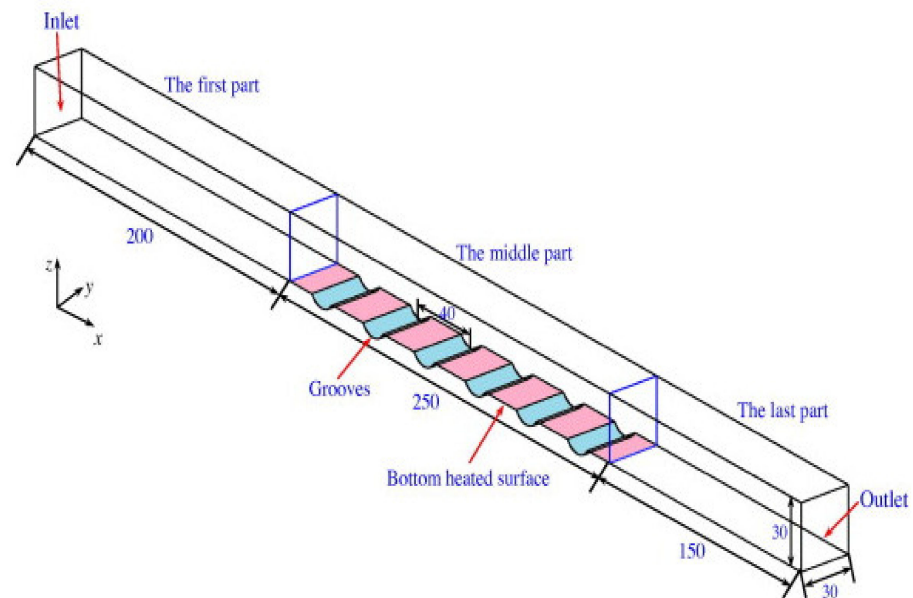
(**a**)
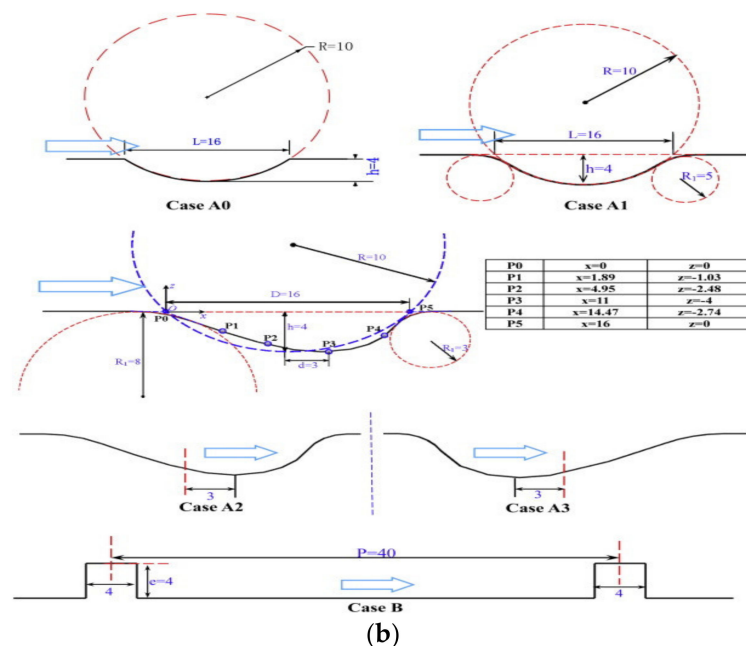
(**b**)

Figure 7. Rectangular micro-channel [83] © Elsevier, 2015; (**a**) geometry description; (**b**) various cylindrical grooves (cases A0–A3) and square ribs (case B).

Zhai et al. [85] simulated the flow in micro-channels with six types of cavities and ribs in the single micro-channel walls. These were "triangular-cavities with circular-rib (a) (Tri.C-C.R for short), (b) triangular-cavities with triangular-rib (Tri.C–Tri.R for short), (c) triangular-cavities with trapezoidal-ribs (Tri.C–Tra.R for short), (d) trapezoidal-cavities with circular-rib (Tra.C-C.R for short), (e) trapezoidal-cavities with circular-rib (Tra.C-C.R for short), (f) trapezoidal-cavities with trapezoid-rib (Tra.C-Tra.R for short)", as seen in Figure 8. De-ionized water was used as a coolant with a Reynolds number ranging from 300 to 600, and a constant heat flux of 10^6 W/m^2 was applied at the bottom wall of the micro-channel. The finite volume method and FLUENT software was adopted to investigate the

flow and heat transfer characteristics. The results showed that using triangular cavities and ribs (see Figure 8f) offered better heat transfer compared to a uniform rectangular micro-channel due to better interaction between the solid and the fluid.
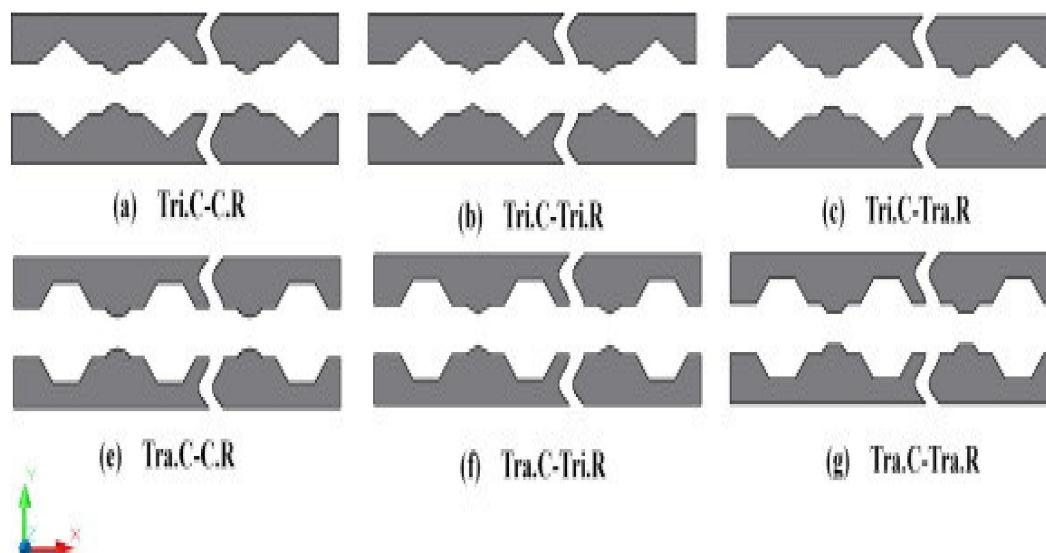

Figure 8. Square channel with different ribs and cavities, (**a**) (Tri.C-C.R), (**b**) (Tri.C–Tri.R), (**c**) (Tri.C–Tra.R), (**e**) (Tra.C-C.R), (**f**) (Tra.C-Tri.R), (**g**) (Tra.C- Tra.R) [86] © Elsevier, 2015.

Knupp et al. [86] proposed a hybrid simulation method to solve the heat transfer and fluid flow characteristics via a single domain strategy and generalized integral transform technique (GITT). This was applied to laminar flow in non-uniform channels, as shown in Figure 9. The results showed that the GITT method was suitable to be applied for Multiphysics applications found to be in good agreement with the finite element calculation form in the commercial software COMSOL Multiphysics, (New York, NY, USA). It is clear that this study agreed well with the literature that using COMSOL Multiphysics provides sufficient agreement with the experimental studies due to the temperature-dependent equations implemented in the software, and it is used widely for solving problems, especially those with Multiphysics applications.
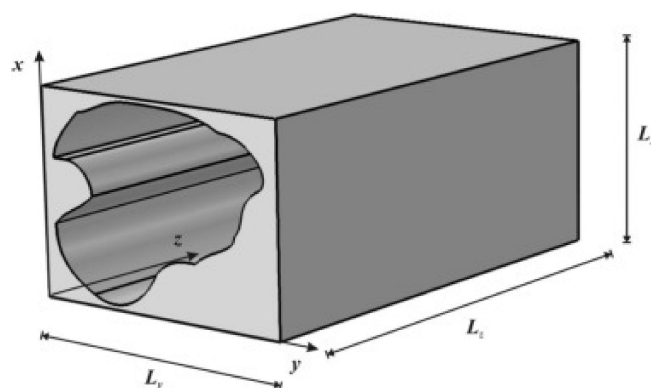
Figure 9. Irregular channel [86] © Elsevier, 2015.

Henze and Wolfersdorf [87] experimentally investigated the impact of tetrahedral VGs on the Nusselt number and the flow velocity. The results showed that using the VGs enhanced the heat transfer rate compared to the uniform channel. In addition, it was found that the highest VGs offered the highest heat transfer enhancement. It was also indicated, as expected, that the heat transfer was enhanced with an increasing Reynolds number.

However, the pressure penalty has not been considered, which determines the pumping power required compared to the uniform channel.

Dai et al. [88] experimentally investigated the influence of zigzag and sine wave micro-channel structures on the laminar water flow and heat transfer maps. They used a Reynolds number in the range of 50 to 900 with heat flux of 19.1 W. A uniform duct was simulated to understand the behavior of hydraulic heat transfer. The results showed that the zigzag geometry enhanced the heat transfer, while the pressure drop increased.

Karathanassis et al. [89] investigated the heat and flow characteristics in an array of fin plate heat sinks. The geometry was designed to be three sections; for each section, the hydraulic diameter was decreased by increasing the number of plates. The FVM was applied to solve the governing equation of the numerical part, while a closed rig with a flow rate ranging from 20 to 40 mL/s was used in the experimental part. It was found that the heat transfer enhanced in the third section due to the buoyancy. Additionally, the temperature was uniform when the Reynolds number decreased. Nevertheless, the pressure drop increased due to an increase in the number of plates.

An analytical investigation has been conducted to study the effect of extended surface area in heat sinks with four types of fins: (a) longitudinal rectangular fin array (LRFA), (b) longitudinal trapezoidal fin array (LTFA), (c) annular rectangular fin array (ARFA), and (d) annular trapezoidal fin array (ATFA), as shown in Figure 10 [90]. The results showed that the triangular fin offered the best heat transfer rate compared to the other three models. It was found that the optimum individual fin was different from the optimum value of heat sink as a component. This is because the individual fin was shorter than the fin in the fins array of the heat sink.
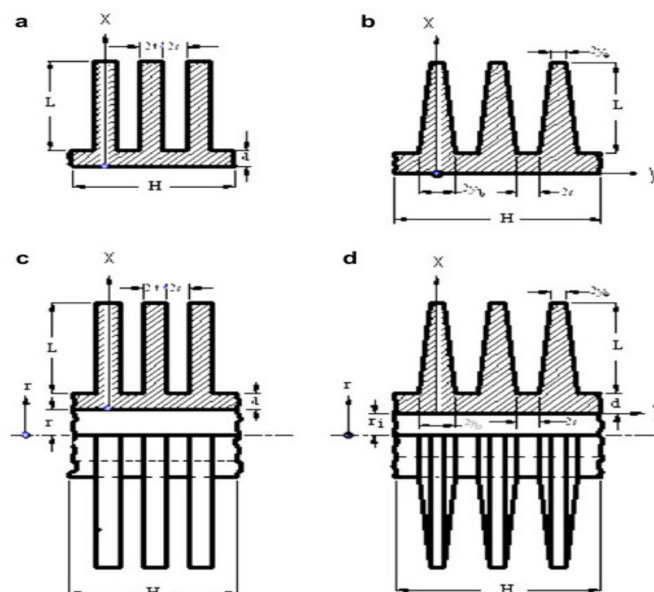
Figure 10. Various types of fins (**a**) LRFA, (**b**) LTFA, (**c**) ARFA, and (**d**) ATFA [90] © Elsevier, 2009.

Ebrahimi et al. [36] studied the impact of using linear VGs to generate vortices in the micro-channel on fluid flow and heat transfer regimes. Different orientations of the VGs and deionized water under laminar flow were considered to simulate three-dimensional geometry utilizing a finite volume method. The results showed that the Nusselt number rose from 2 to 25% when the Reynolds number ranged from 100 to 1100. However, the friction factor increased by up to 30% when using longitudinal VGs. This friction factor penalty could be acceptable if the space was limited and a certain heat transfer rate had to be achieved.

Hong et al. [91] sought to improve the uniformity of the temperature distribution in micro-channel heat sinks by considering a heat sink in which the micro-channels formed a rectangular fractal-shaped network. Their numerical analysis of the 3D conjugate heat

transfer revealed hotspots in regions where the channel density was sparse; however, these could be overcome by local modifications of the channel size. The modified network was found to have lower thermal resistance, lower pressure drop, and much improved uniformity in temperature compared to parallel-channel heat sinks.

A recent study carried out by M. Al-Asadi and M. Wilson [1] examined different geometries of perforated pin-finned heat sink. The study examined a perforated pin-finned heat sink using air and water. The results showed that the perforated pin-finned heat sink offered better heat transfer performance and lower pressure penalty compared to a solid pin-finned heat sink when using air as a working fluid, whilst no enhancement was gained when using water due to the high viscosity of the water. The study also compared different shapes of vortex generators such as rectangular, triangular, and circular VGs in a uniform channel. The results conducted that the circular VG was the best in enhancing heat transfer among the examined shapes.

From the previous two sections, it can be seen that there is a gap in the knowledge of different shapes of VGs, especially in cylindrical vortex generators. Thus, the next section focuses on cylindrical vortex generators.

3.2. Cylindrical Vortex Generators

The above examples show that there are many ideas for geometrical modifications of micro-channels, some of which are rather complex. A somewhat simpler yet still effective class of geometrical modifications are ribs or cylinders added to the channel walls, base, or interior. These act as transverse vortex generators and have been shown to enhance the heat transfer [34,92–96].

A two-dimensional numerical study by Cheraghi et al. [45] considered a smooth channel with fixed heat flux through the wall sides and an adiabatic cylinder at various locations inside the channel. The Reynolds number was 100 and Prandtl number ranged from 0.1 to 1. The authors found that the maximum enhancement occurred when the cylinder was fixed halfway from the base to the top of the channel. The results also showed that the low Prandtl number had a positive effect on heat transfer enhancement.

Turbulent flow in a channel with cylindrical vortex generators was investigated numerically by Wang and Zhao [97]. It was found that utilizing a cylindrical vortex generator enhanced the heat transfer by 1.18 times compared to the corresponding uniform channel. However, this study did not take into account the thermal conductivity of the rib, which might distribute the heat to the fluid due to the high thermal conductivity of metals compared to fluids, resulting in further enhancement of the heat transfer in micro-channels.

Chai et al. [98] numerically investigated the effects of ribs on the side walls of a silicon micro-channel heated from below and cooled by laminar water flow. The ribs were arranged in an offset manner on both side walls, and had various cross-sectional shapes, namely rectangular, backward triangular, forward triangular, isosceles triangular, and semi-circular, each with a protrusion of 25 µm into the channel. For a Reynolds number in the range of 190–838, Nusselt numbers up to 1.95 times that of a smooth channel were achieved, with the apparent friction factor increasing up to 4.57 times. Performance evaluation criteria values of 1.02 to 1.48 were found, with forward triangular ribs performing best for Re < 350, and semi-circular ribs for Re > 400. In a further three-part work, the same authors also studied aligned versus offset fan-shaped ribs on the opposite side walls [99–101]. Various other side-wall rib shapes and configurations have also been considered by others, e.g., [102,103].

Al-Asadi et al. [104] studied the influence of cylindrical VGs with radii up to 400 µm on 3D conjugate heat transfer. In particular, VGs with quarter- and half-circular cross-sections attached at the base of the micro-channel were considered, aligned perpendicular to the flow direction, with an input heat flux in the range of 100–300 W/cm^2 and a Reynolds number ranging from 100 to 2300. While the quarter-circle VGs offered no improvement in heat transfer, the half-circle cylindrical VGs provided a reduction in the thermal resistance of the system. In addition to VGs completely spanning the width of the micro-channel, shorter VGs were also considered. It was found that having a gap between each channel

wall and the ends of the VGs offered further heat transfer benefits, particularly when the pressure drop penalty was taken into account, though the underlying mechanisms by which the gaps enhanced the performance were not explored.

Furthermore, Al-Asadi et al. [8] continued to investigate the influence of the gap in detail in their recent study. It was found that the gap of 75 μm at each end offered the highest heat transfer performance but a lower PEC index compared to the VG with a central gap of 450 μm.

A vortex generator in a uniform heat sink enhances the heat transfer but offers a high pressure drop. The heat transfer enhancement increases with the radius of the VGs. However, Al-Asadi et al. [105] confirmed that the largest VGs do not offer a high PEC.

4. Nanofluids Overview

As remarked in the introduction, an alternative to modifying the geometry to enhance the heat transfer is to modify the working fluid. The last decade has seen a dramatic increase in the nanofluids, as can be seen in Figure 11. Compared to previous years, it is expected that there will be more publications this year as the data are only from up to April 2018.
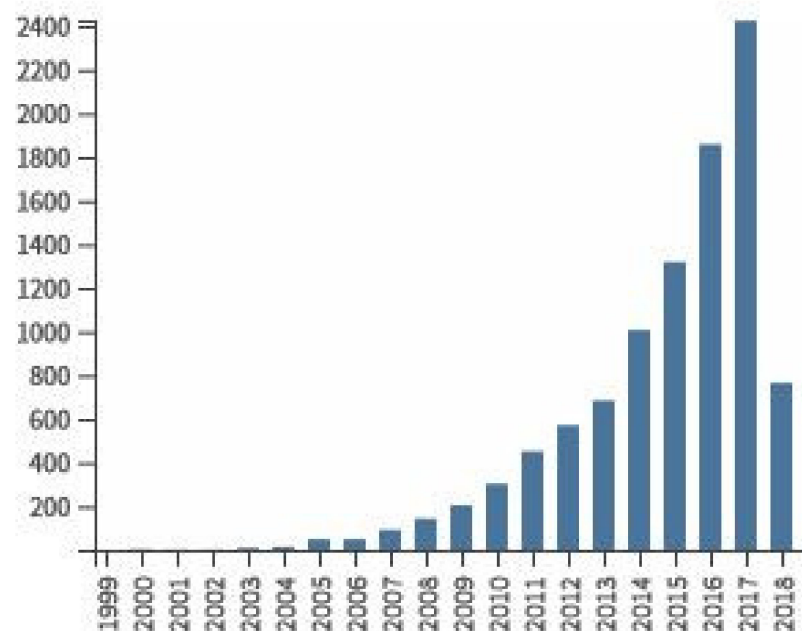
Figure 11. Growth of publications in nanofluids [77] © Elsevier, 2017.

Using nanofluids increases the pumping cost to drive the flow of cooling systems. Thus, researchers have extensively studied the effects of nanofluids on conjugate heat transfer in various ways, such as the effect of fluid temperature, nanoparticle shape, clustering of nanoparticles, and the effect of pH (potential of hydrogen). However, the most related factors to this study are explained below.

4.1. Nanofluids Preparation

A nanofluid is a solid–liquid combination fluid obtained by dispersing nano-sized particles up to 100 nm in a base fluid to improve thermal conductivity of the base liquid [106–109]. Nanofluids can be prepared using several approaches such as a single-step method and two-step method.

The single-step method is a direct evaporation method by which nanoparticles are dispersed directly into a working fluid. In 1996, this method was used to prepare Al_2O_3 and CuO nanoparticles by Eastman et al. in Argonne National Laboratory in the USA [110]. The same procedure was employed by Lee et al. [111], Choi and Eastman [112], and

Choi et al. [113]. After this, Zhu et al. [114] produced Cu-ethylene glycol nanofluid from copper sulphate anhydride ($CuSO_4 \cdot 5H_2O$) and sodium hypophosphite ($NaH_2PO_2 \cdot H_2O$) reaction under microwave irradiation. This one-step method produced nanofluid with good stability.

In a two-step procedure, the first step introduces an inert gas to produce a dry powder of nanoparticles. These nanoparticles are then dispersed in the conventional fluid. Li and Xuan [108] used the inert gas method, which can produce clean nanoparticles and, as a result, produce a stable nanofluid. However, this method is difficult and expensive for nanoparticle requirements. Consequently, many other techniques may produce dry nanoparticles, such as chemical techniques [115], the aerosol spray method [116], metal vapor [117], arc discharge for nano-carbon tubes [118,119], laser ablation [120], a catalytic process [121], or another successful method called the VEROS (vacuum evaporation on running oil substrate) method [122]. In this technique, direct evaporation in a vacuum onto the surface of running oil was used to produce nanoparticles in small size (10 nm). However, the VEROS technique is not suitable for substances of more than one component, such as metal oxides, and the separation of nanoparticles from the fluid is difficult to produce the dry nanoparticles. The VEROS method was modified by Eastman et al. [123]; they replaced the oil by ethylene glycol to produce Cu-ethylene glycol nanofluid.

4.2. Thermo-Physical Properties of Nanofluids

Nanofluids have high thermo-physical properties [124]. As a result of having high thermal conductivity, nanofluids can offer high heat transfer performance compared to the base fluid without nanoparticles. Various considerations of nanofluid properties have been made to evaluate and prepare nanofluids, such as the effect of base fluid, dispersion and distribution [125], particle shape [126,127], volume concentration [128–131], particle-shell structure [132,133], and thermal contact resistance [134,135]. Furthermore, different factors affect the heat performance of nanofluids such as thermal conductivity, density, viscosity, and heat capacity.

Nanofluids can be used with different shapes of different channels to enhance the heat transfer; for example, a V shape wavy plate channel was studied numerically using various types of nanoparticles and base fluids [136]. The study used a large range of Reynolds number from 8000 to 20,000. The FVM was used to solve the governing equation with the k–ε standard turbulent model to investigate the heat transfer performance. It was found that the best nanofluid was silicon oxide particles in glycerin base fluid to enhance the Nusselt number. However, the pressure drop increased using nanofluids. Such studies should consider an optimization of the heat transfer enhancement and pressure drop increase; a simple optimization factor such as the hydraulic thermal performance also gives an indication about overall enhancement [104].

4.2.1. Experimental Data of Thermal Conductivity

Investigators focused on providing comprehensive data of thermal conductivity and the factors which play a major role to enhancing the thermal conductivity of nanofluids. They found that the base fluid, nanoparticle size, material, and concentration are the most effective parameters. Therefore, Table 1 illustrates a brief survey of thermal conductivity studies.

Table 1. Heat transfer enhancement using different fluids.

Base Fluid	Particles	Size [nm]	φ%	Enhancement
Water [12]	Al_2O_3	30	0.3–2	h > 57%, Nu = 62%
Water [110]		33	5	29%
Water [111]		24.4, 38.4	4	10%
EG			5	17%

Table 1. *Cont.*

Base Fluid	Particles	Size [nm]	φ%	Enhancement
Water [137]		28	3	12%
EG			8	40%
EO			7	50%
Water [138]		38.4	4	24.3%
Water, EG, PO [139]		12.2–302	5	30%
Water [140]		36	10	29%
Water [141]		27–56	1.6	10%
Water [142]		48	1	4%
Water [143]		20	14.5	20%
Water [144]		110–210	1	0%
Water [145]		36, 47	6	28%
Water [146]		8–282	4	18%
EG		12–282	3	16%
Water [147]		36, 47	18	30%
Water	CuO	36	5	60%
Oil			5	44%
Water [111]		18.6, 28.6	3.5	12%
EG			4	20%
Water [137]		23	4.5	12.3%
EG			6	12.5%
Water [138]		28.6	4	36%
Water [139]		29	6	58%
Water [143]		33	5	18%
Water [142]		33	1	5%
EG			1	9%
Water [147]		29	3.3	8%
Water [148]		L = 50–100	0.4	9.6%
Water [149]	TiO$_2$	10,15 -40 rod	5	30, 33%
Water [150]		165	0.72	6.5%
Water [143]		40	2.5	6%
Water [151]		95	2	22%
Water [142]			1	14.4%
Water [152]			3	9.6%
Water [153]	Fe$_3$O$_4$	9.8	5	38%
EG [142]	WO$_3$	38	0.3	14%
Water [143]	ZrO$_3$	20	10	15%
Water [144]		110–250	0.1	0%
Water [144]	SiO$_2$	20–40	0.1	0%
Water [154]		12	1	3%
EG [155]	Cu	<10	0.3	40%
Water [156]		100	7.5	75%

Table 1. *Cont.*

Base Fluid	Particles	Size [nm]	φ%	Enhancement
Oil			7.5	44%
Water [157]		50–100	0.1	23.8%
EG [158]	Fe	10	0.55	18%
EG [159]		10	0.2	18%
EG [142]		10	0.55	18%
Water [160]	AG, Au	10–20	0.001	4%
Toluene			0.001	9%
Toluene [161]	Au	2	0.04	1.5%
Ethanol		4	0.03	1.4%
Toluene	Fullerene C60-C70	0.5–0.6	0.8	0%
Mineral oil [161]		10	0.8	6%

Increase in the thermal conductivity of the working fluid improves the efficiency of the associated heat transfer process. However, investigations into the convective heat transfer of nanofluids indicated that the enhancement of heat transfer coefficient exceeds the thermal conductivity enhancement of nanofluids [162–165]. Moreover, other parameters such as the density, heat capacity, and viscosity have a lower effect than thermal conductivity.

4.2.2. Theoretical Development of Nanofluid Equations

Investigators have started from the Maxwell equation [166] to predict the thermal conductivity of nanofluids. Improving the Maxwell equation offered a better understanding of the behavior of thermal conductivity since 1935, when Bruggeman [167] reported that a high concentration of nanoparticles cannot be neglected. Moreover, in 1987, Hasselman [135] modified the theory of Maxwell considering the size of the composite dispersed phase in addition to the volume concentration. However, these studies under-predicted the experimental measurements.

Many investigations have tried to improve the Maxwell equation to produce a modified thermal conductivity equation that offers good agreement with the experimental data. Modern techniques were utilized to enhance the prediction of nanoscale equations such as the nanoparticle–matrix interfacial layer [168,169], nanoparticle Brownian motion [170,171], and nanoparticle cluster/aggregate [172].

Nie et al. [173] used the exact expression for the heat flux vector of the base fluid plus a nanoparticle system to estimate the contribution of nanoparticle Brownian motion to thermal conductivity. It was found that its contribution is too small to account for the abnormally high reported values. The mean free path and the transition speed of phonons in nanofluids were estimated through density functional theory. It was found that a layer structure can form around the nanoparticles and the structure does not further induce fluid–fluid phase transition in the bulk fluid.

In contrast to Nie et al. [152], Ghasimi and Aminossadati [174] showed that considering Brownian motion would enhance the thermal conductivity. They used CuO-water nanofluid in a right triangular enclosure. The results also reported that heat transfer was enhanced with the increase in nanoparticles.

Xuan and Roetzel et al. [175] suspended ultrafine particles to change the properties and heat transfer performance of the nanofluid, which exhibited a great potential in enhancing the heat transfer. Based on the assumption that the nanofluid behaves more like a fluid than a conventional solid–fluid mixture, they proposed two different approaches for deriving the heat transfer correlation of the nanofluid. The effects of transport properties of the nanofluid and thermal dispersion were also included.

4.2.3. The Effect of Base Fluid

The base fluid can be water, oils, or ethylene glycol. Researchers have investigated the effect of base fluid on heat transfer enhancement for two decades [176–178].

Xie et al. [179] studied the enhancement ratio of thermal conductivity between the base fluids and nanofluids. They considered three types of base fluid (water, glycerol, ethylene glycol and pump oil) with α-Al$_2$O$_3$ nanoparticles. The results showed that the water-based nanofluid had the lowest thermal conductivity compared to other nanofluids, while the thermal conductivity of the water itself was higher compared to the other base fluids.

However, using nanofluids with water-based nanofluid was most common in many heat-transfer and fluid-flow applications.

4.2.4. The Effect of Nanoparticles Concentration

The influence of the concentration is an effective factor to enhance the thermo-physical properties of nanofluids. It is the portion of volume of nanoparticles to the base fluid. Many researchers declared that having solid particles in the base fluid would enhance the thermal conductivity of nanofluids, increasing the viscosity and density of nanofluids [177,180–185]. Furthermore, nanofluids showed non-Newtonian behavior when using nanoparticles of more than 5% [165,186]. However, due to the high thermal conductivity of metallic nanoparticles, they offer the highest thermal conductivity of nanofluids compared to the oxides and non-metallic nanoparticles. Yulong et al. [187,188] studied the effect of volume concentration on thermal conductivity enhancement. They found that the thermal conductivity enhanced with the nanoparticles, as shown in Figure 12.
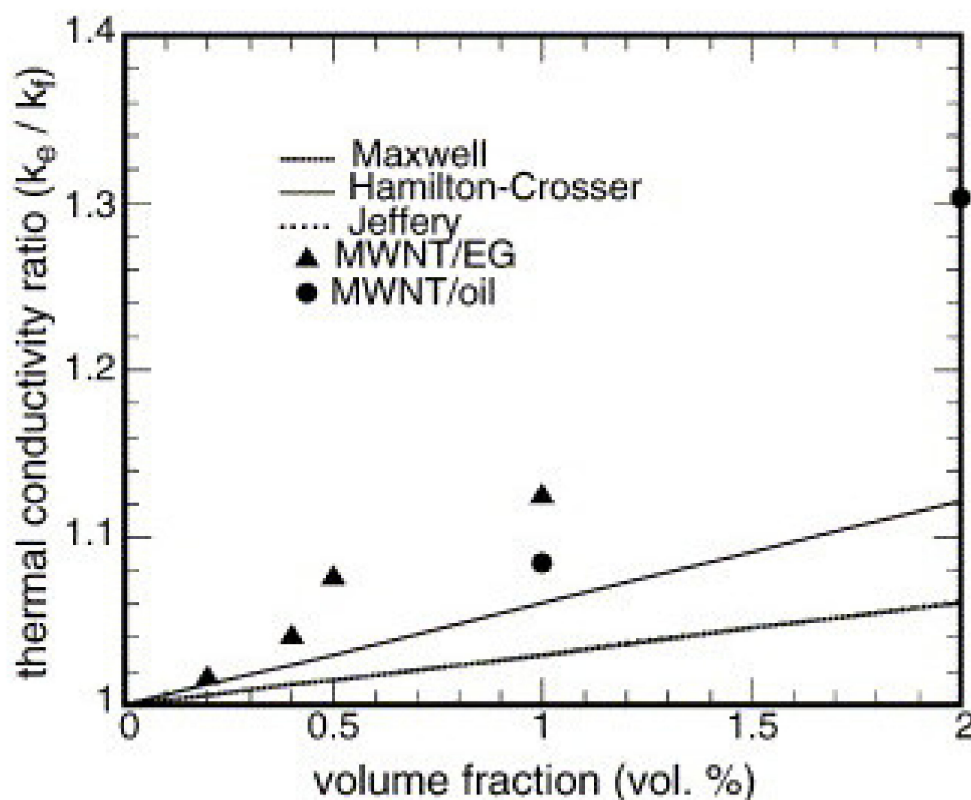

Figure 12. The influence of nanoparticle concentrations on thermal conductivity.

Another study by Kumar et al. [189] investigated the impact of thermal conductivity and base fluid on conjugate heat transfer. They utilized CuO and TiO$_2$ up to 1% of volume concentration and different base fluids of water and ethylene glycol under a temperature ranging from 30 to 50 °C. The study found that the thermal conductivity enhanced as the nanoparticle concentration increased for both cases; an example is shown in Figure 13. The very famous study on thermal conductivity carried out by INPBE [190] reported

that the enhancement relationship between the thermal conductivity and nanoparticles concentration was approximately linear.
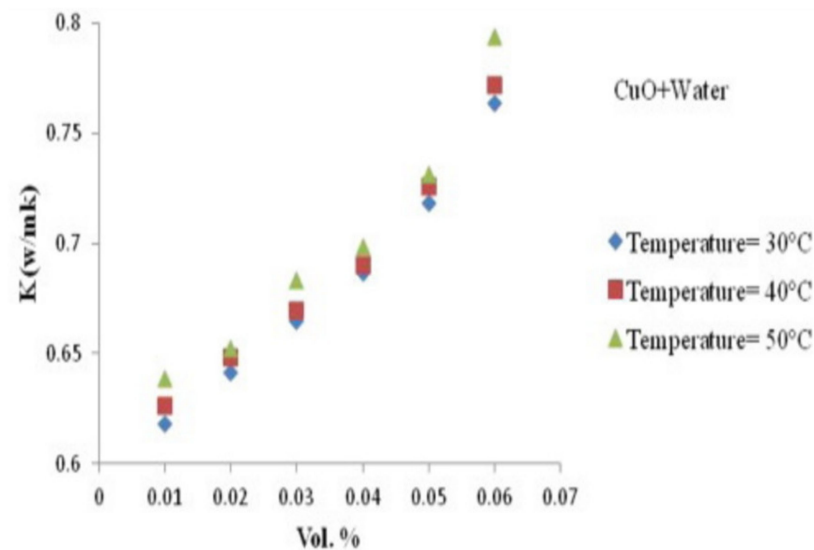

Figure 13. The influence of nanoparticle concentrations on thermal conductivity [189] © Elsevier, 2016.

4.2.5. The Influence of Nanoparticle Materials

As one might expect, the nanoparticle material has an effect on resulting nanofluid properties. Nanoparticles can be metallic (Fe, Cu, Ag, Au, Al), carbon or metallic oxide (Fe_3O_4, CuO, Al_2O_3, TiO_2, SiC, SiO_2, ZnO) [191–195]. Metallic oxide nanoparticles are commonly used with water as a base fluid. This is because the oxides are considered more stable than the pure metals in fluids. Moreover, the oxygen in the dioxides makes nanoparticles disperse easily and stable in the base fluid. However, Al_2O_3 and SiO_2/water nanofluids offer the highest heat transfer enhancement among the common nanofluids. Some researches have indicated that SiO_2/water nanofluids offer higher heat transfer enhancement compared to Al_2O_3/water [184,196–198], while others have reported the opposite findings [199–201].

4.2.6. Thermal Conductivity

The thermal performance of a working fluid can be enhanced by increasing its thermal conductivity. This is because solid nanoparticles have higher thermal conductivity than the base fluid; for instance, at room temperature, the thermal conductivity of copper is 700 times higher than that of the water. Therefore, adding solid nanoparticles to the base fluid improves the thermal conductivity of the working fluid. A ratio between the nanofluids and the base fluid can be applied k_{nf}/k_{bf} to calculate and evaluate the enhancement of the thermal conductivity of nanofluids. The enhancement of thermal conductivity achieved 40% in some cases, despite the concentration of the nanoparticles not exceeding 10% [110,113,137,138,140,155,202].

In the last two decades, some researchers have indicated that there was no agreement between the theoretical equations and experimental data in terms of thermal conductivity, while Keblinski et al. [203] reported that most results of numerical and experimental investigations showed good agreement. However, the study by Keblinski et al. [203] was supported by a benchmark study of thermal conductivity carried out by the International Nanofluid Properties Benchmarking Exercise (INPBE) [190]. The INPBE sent samples to 30 organizations worldwide to measure the thermal conductivity. The results showed that the thermal conductivity showed $\pm 10\%$ or lower average differences between the experimental data and theoretical equation of thermal conductivity. Nanofluids have high thermo-physical properties compared to the base fluid in terms of thermal conductiv-

ity [204–208] and heat transfer coefficient [209–211]. Therefore, theoretical and experimental surveys are presented in the next sections.

4.3. Nanofluid Equations

4.3.1. Thermal Conductivity

Modern equations of effective thermal conductivity [212] are presented based on the basic correlation [213], which was developed [214] to be two equations: static and Brownian thermal conductivity (see Equation (1)). The static thermal conductivity is proposed by [174] (see Equation (2)) as below:

$$k_{eff} = k_{static} + k_{brownian} \tag{1}$$

$$k_{stattic} = k_f \left[\frac{(k_s + 2k_f) - 2\varphi(k_f - k_s)}{(k_s + 2k_f) + \varphi(k_f - k_s)} \right] \tag{2}$$

where k_s and k_f are the thermal conductivities of the particles and the fluid, respectively.

The Brownian motion thermal conductivity equation [214] is:

$$k_{brownian} = 5 \times 10^4 \beta \varphi \rho_f Cp_f \sqrt{\frac{KT}{\rho_s d_s}} f(T, \varphi) \tag{3}$$

where:

$$f(T, \varphi) = \left(2.8217 \times 10^{-2}\varphi + 3.917 \times 10^{-3}\right)\left(\frac{T}{T_0}\right) + \left(-3.0669 \times 10^{-2}\varphi - 3.91123 \times 10^{-3}\right)$$

where K is the Boltzmann constant, T is the fluid temperature, and T_0 is the reference temperature.

4.3.2. Viscosity Equation

The viscosity of the nanofluid is approximately the same as the viscosity of a base fluid if containing dilute suspension of fine spherical particles, as shown below [174]:

$$\frac{\mu_{eff}}{\mu_f} = \frac{1}{1 - 34.87 \left(d_p/d_f\right)^{-0.3} \varphi^{1.03}}$$
$$d_f = \left[\frac{6M}{N\pi\rho_{fo}}\right]^{1/3} \tag{4}$$

where μ_{eff} and μ_f are the viscosity of nanofluid and base fluid, respectively, d_p is the nanoparticle diameter, d_f is the base fluid equivalent diameter, and φ is the nanoparticles volume fraction. M is the molecular weight of the base fluid and N is the Avogadro number, and ρ_{fo} is the mass density of the base fluid calculated at temperature T = 293 K.

4.3.3. The Density Equation

The effective density consists of three main parameters, which are the nanofluid concentration (φ), nanoparticle density ρ_s, and base fluid density ρ_f [12]:

$$\rho_{eff} = (1 - \varphi)\rho_f + \varphi\rho_s \tag{5}$$

4.3.4. The Effective Heat Capacity Equation

With Cp_s being the heat capacity of the solid particles, and Cp_f being that of the base fluid, the effective heat capacity of the nanofluid is given by [183]:

$$(Cp)_{eff} = \frac{(1 - \varphi)(\rho Cp)_f + \varphi(\rho Cp)_s}{(1 - \varphi)\rho_f + \varphi\rho_s} \tag{6}$$

4.3.5. The Effective Thermal Expansion Equation

The thermal expansion for solid parts β_s and for base β_f fluid with φ can produce the effective thermal expansion as follows [215,216]:

$$\beta_{eff} = \frac{(1-\varphi)(\rho\beta)_f + \varphi(\rho\beta)_s}{(1-\varphi)\rho_f + \varphi\rho_s} \qquad (7)$$

4.4. Drawbacks of Nanofluids

Recent investigations have indicated that there is no benefit to using nanofluids. Moreover, Myers et al. [217] revealed that there is a lack of consistency between the mathematical and experimental studies. The authors also indicated that comparing nanofluids on the basis of non-dimensional parameters such as the Reynolds number is misleading in drawing a correct conclusion on the real heat transfer enhancement. Furthermore, Haddad et al. [218] reviewed natural convection using nanofluids. They indicated that in numerical studies the heat transfer was significantly enhanced using nanofluids; nevertheless, the experimental investigations showed the opposite results. However, this study reviewed the natural convection investigations only, which can support the opposite results of the experimental studies because there is perhaps not enough flow to circulate the nanoparticles in the system, which leads to augmentation of the nanoparticles in one place of the system. This could cause hot spot zones, decreasing the heat transfer performance of the system. The reason behind the discrepancy between the numerical and experimental studies of the same working condition might be the augmentation, as the numerical studies do not take this issue into account.

Another point of using a fixed Reynolds number and a fixed pumping power with nanofluids was highlighted by Haghighi et al. [219]. The results showed that there is no enhancement in heat transfer when using a fixed pumping power with nanofluids. However, using a fixed Reynolds number showed good enhancement of heat transfer. The same findings were concluded by Alkasmoul [220,221].

Though nanofluids enhance the heat transfer rate, they attract more cost in pumping to drive the fluid [210,222–227].

There are other applications that indicate that water-based nanofluids cannot offer any benefit for cooling systems because of the high temperature conditions; for instance, semiconductor materials such as silicon carbide (SiC) and gallium nitride (GaN) operate under special temperature conditions above 200 °C [228]. In this case, nanofluids do not offer any option to enhance the heat transfer performance due to the limitation of the temperature condition. Therefore, a replacement fluid should be used to overcome this issue. The solution might be by suggesting another advanced liquid which has different chemical properties to the nanofluid. This advanced fluid could be an ionic liquid which works with high heat flux [229].

5. Evaluation of Heat Transfer Improvement

In electronics, the main aim of enhancing a cooling system is to reject the generated heat and keep the electronics working in the range of a limited temperature of 85 °C [104]. Recently, optimizing the energy to reduce the power consumption of the cooling system has attracted many researchers; the power consumption could be the pumping power of the cooling system or the power reduction after enhancing the cooling system.

To help to evaluate the benefit reuse cost of a proposed modification of a cooling system, a performance evaluation criterion (PEC) index can be formulated which accounts for both change in heat transfer performance and fluid flow effects [230,231]. The heat transfer term could be the Nusselt number or thermal resistance, while the fluid flow term might be the friction factor or pressure drop. This formula can be used to evaluate the performance of the overall enhancement of the system.

Furthermore, the formula could be used to evaluate the performance of modification of the geometry by comparing basic and developed designs such as a smooth and modified micro-channel, as shown in the equation below [29,30]:

$$PEC = \frac{Nu/Nu_s}{(f/f_s)^{1/3}} \tag{8}$$

where Nu, Nu_s are the Nusselt numbers for modified and straight channels, and f, f_s are the friction factor for modified and straight channels.

An example of the importance of the PEC is the study by Al-Asadi et al. [8], which indicated that the heat transfer was enhanced (the thermal resistance is reduced) using cylindrical VGs with a central gap of 100 µm but higher pressure drop than the cylindrical VGs with an end gap. However, the results were reversed (cylindrical VGs with an end gap offer better heat transfer than the cylindrical VGs with a central gap of 100 µm) when taking the pressure drop into account using PEC.

This evaluation method was used by many researchers to examine the performance of the proposed designs. Furthermore, it could be considered as a starting point for optimizing the whole system.

6. Validation of Numerical Methods Versus Experimental Investigations

Developments in numerical solution methods for heat transfer in the system have made them more accurate and more closely aligned with the experimental data, for example, considering the temperature dependence of the thermo-physical properties [104]. Many investigations have been carried out to improve the numerical methods, such as the study by Bushehri et al. [232], who proposed a new method to deal with fluids and solids with an equation utilizing the (FVM) CFD software openFOAM, (New York, NY, USA) with new boundary conditions for the temperature jump and flow slip. The equation was tested against previous works and showed good agreement. It was applied to a micro-channel heat sink consisting of two parallel plates to investigate the heat transfer performance. The results indicated that the heat transfer was accurately calculated using the proposed equation.

Moreover, many studies have paid attention to numerical simulation because it is important to predict the experimental measurements such as heat flux, temperature, and fluid velocity. Using simulation offered a low cost compared to the experimental setup [67]. Many investigations have also developed the numerical methods, making them more accurate and efficient, for instance, improving a hybrid finite element method to solve solid–liquid equations of the microchannel [233], as well as modifying a technique such as the generalized integral transform technique (GITT) to solve the coupling equation, which showed very good agreement with the COMSOL Multiphysics® [234].

An example of good agreement between the numerical and experimental studies can be seen in Figure 14.

However, Al-Asadi et al. [1,8] showed that using governing temperature-dependent equations for thermal properties gives better results than temperature-independent equations. The temperature dependence of the fluid properties is given by the following expressions built into COMSOL based on experimental data:

$$\rho(T_L) = 838.466135 + 1.40050603T_L - 0.0030112376T_L^2 + 3.71822313 \times 10^{-7}T_L^3 \tag{9}$$

$$\mu(T_L) = 1.3799566804 - 0.021224019151T_L + 1.3604562827 \times 10^{-4}T_L^2 - 4.6454090319 \times 10^{-7}T_L^3$$
$$+8.9042735735 \times 10^{-10}T_L^4 - 9.0790692686 \times 10^{-13}T_L^5 + 3.8457331488 \times 10^{-16}T_L^6 \tag{10}$$

$$C_P(T_L) = 12010.1471 - 80.4072879T_L + 0.309866854T_L^2 - 5.38186884 \times 10^{-4}T_L^3 + 3.62536437 \times 10^{-7}T_L^4 \tag{11}$$

$$k(T_L) = -0.869083936 + 0.00894880345T_L - 1.58366345 \times 10^{-5}T_L^2 + 7.97543259 \times 10^{-9}T_L^3 \tag{12}$$
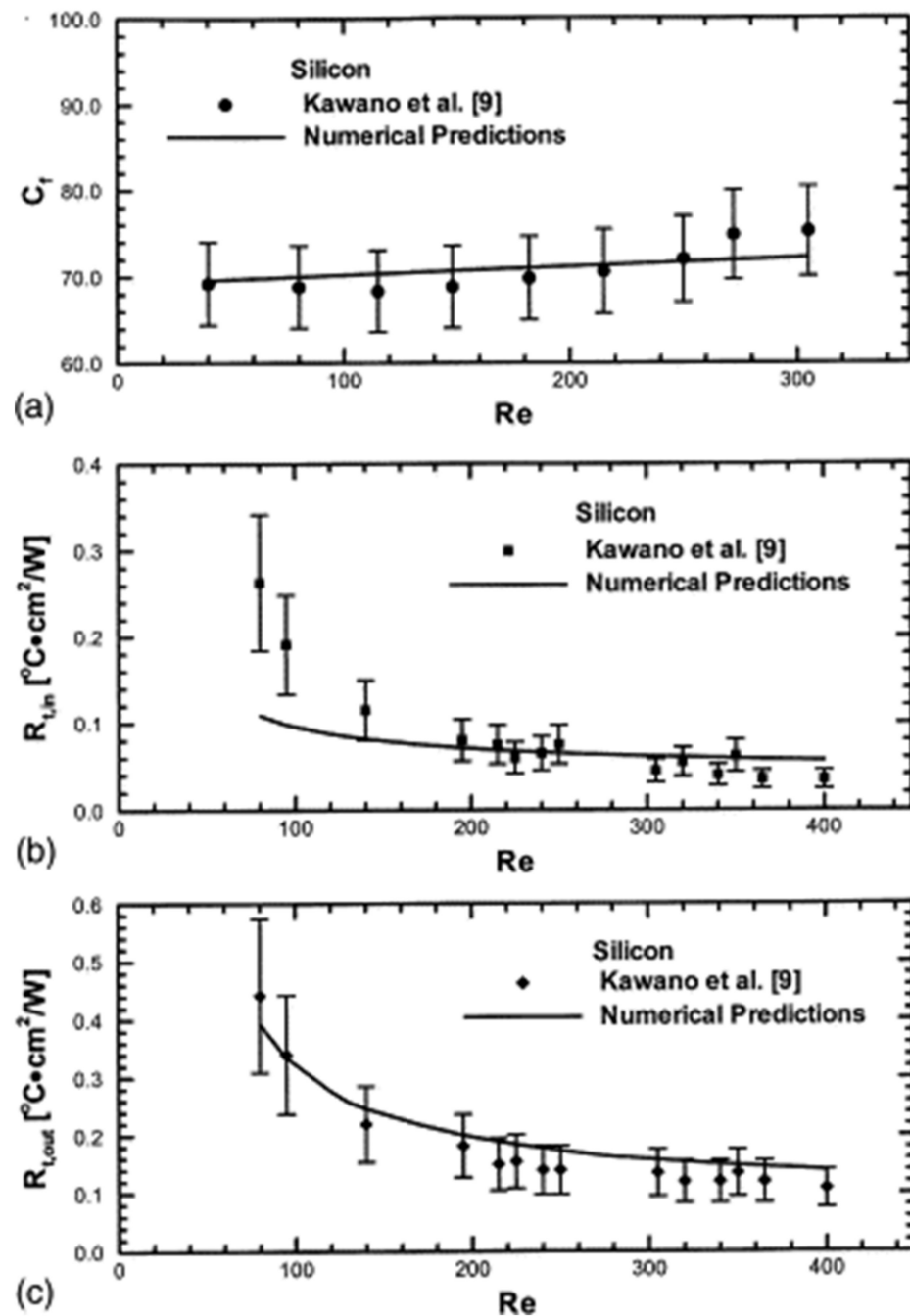
Figure 14. Validations between numerical findings of Qu and Mudawar [235] © Elsevier, 2002 and experiments of Kawano et al. [236] © Elsevier, 1998; (**a**) friction coefficient, (**b**) inlet thermal resistance, and (**c**) outlet thermal resistance.

It was found that applying the above equations used by Al-Asadi et al. [1,8] produces better results compared to the experiments of Kawano et al. [236] as presented in Figure 15.
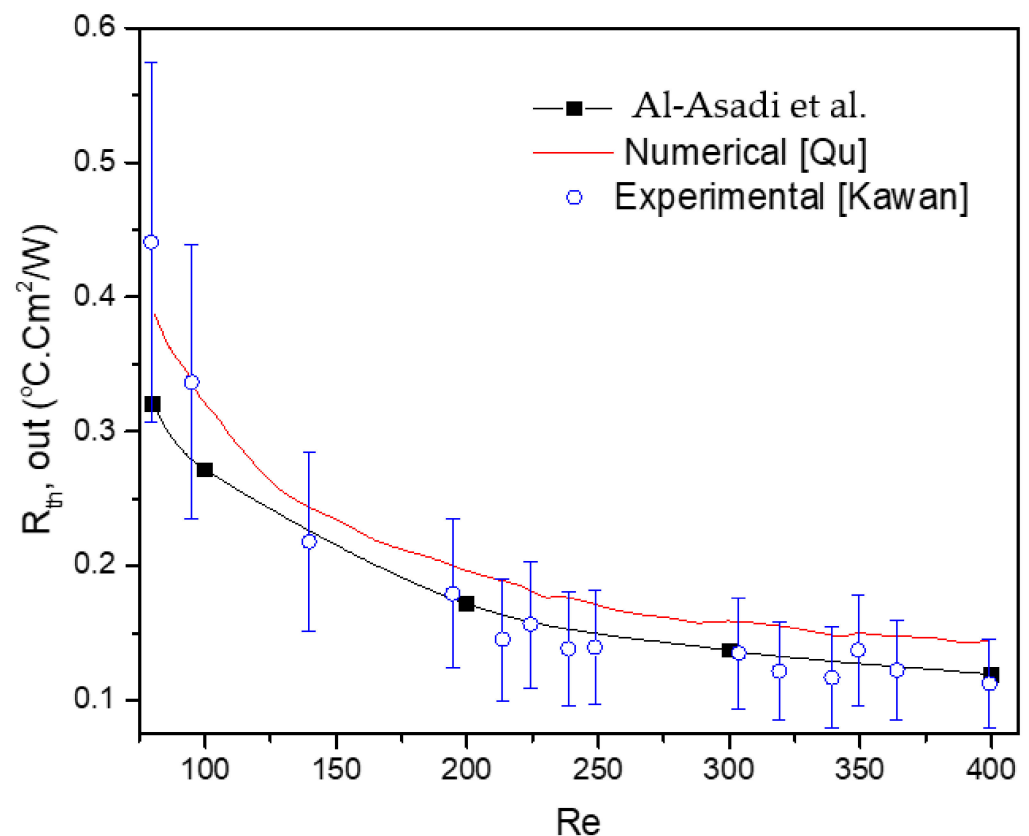
Figure 15. Validation of the present model against experimental data of Kawano et al. [236] © Elsevier, 1998 and alternative numerical results of Qu and Mudawar [235] © Elsevier, 2002 and Al-Asadi et al. [1,8].

7. Conclusions and Recommendations for Future Work

A comprehensive literature review has been provided in this paper to understand the gaps in knowledge in the available literatures on micro-channel heat sink and nanofluids investigations. Numerous experimental configurations and theoretical studies have been devoted to investigating the variety of geometry designs such as straight, curved, regular, irregular, extended surface, and vortex generators (VGs) to enhance the heat transfer and fluid flow. Attempts at improvement included the use of different micro-channel geometries, coolant types, and structural materials. Any improvements in the overall performance of the systems were analyzed using different analysis methods. As a result, several conclusions can be drawn, summarized as follows:

- All studies in the literature indicated that using extended surface areas such as ribs or grooves in uniform channels offered better heat-transfer enhancements compared to the uniform channels themselves. However, there will be a pressure drop penalty caused by ribs and grooves disturbing the fluid flow. Thus, the modified channels are a recent area focused especially on using VGs as their influence on heat transfer and fluid flow characteristics. Two types of vortex generators (VG) have been classified based on the direction of the axis of rotation of the vortices generated, which were transvers and longitudinal VGs.
- Although there are many examples of geometrical modifications that offer some form of benefit in terms of heat transfer, most of these are rather complex. So far, simpler cylindrical vortex generators have only been explored partially in two recent studies. However, they have focused on flow disturbance, treating the VGs as adiabatic objects; therefore, conjugate heat transfer effects have not been precisely considered.
- Based on the available literature, there are few numerical studies of mini- or micro-channels using cylindrical vortex generators [1,8,45,97,104,227], while no experimental

investigation has been found; this is because of the limitations of manufacturing micro-sized channels. However, the literature has shown good agreement between the numerical and experimental studies for mini-channels. Thus, the motivation for this review paper was to highlight the modified design of different shapes of VGs.

- Another aspect by which the heat transfer in micro-channels can be enhanced is by using a nanofluid. However, the price is paid for the pumping power. The literature showed that there is an argument when comparing SiO_2 and Al_2O_3 nanoparticles in water at the same concentration: some researchers revealed that the Al_2O_3 water offers better heat transfer enhancement, whereas others indicated the opposite. However, there are still areas of disagreement in terms of the benefit of using them. Although the thermal conductivity can be enhanced, the drawback of nanofluids is the increases in pressure drop required to drive the flow. Thus, deeper investigation has been carried out and highlighted in this paper to study the performance of these two types of nanofluids.

- Other ideas have focused on modifications within the parallel channels themselves—for example, by adding grooves or ribs [29–32]. They act as vortex generators (VGs) to enhance the heat transfer and fluid flow characteristics by disturbing the flow and creating vortices that can be classified as transverse vortices, where the axis of rotation is perpendicular to the flow direction, or longitudinal vortices, with axes lying along the direction of flow. Longitudinal vortices are generally more effective than transverse ones in enhancing the heat transfer performance [16,33,237]. VGs can take various forms, such as protrusions, wings, inclined blocks, winglets, fins, and ribs [2,36,103,238], and have also been used to enhance heat transfer in different geometries such as circular and non-circular ducts under turbulent flow [19,34,239]. They have also been used in laminar flow [41], with flat plate-fins in rectangular channels [37–39], tube heat exchangers [40], heat sinks [41,42], and narrow rectangular channels [43,44]. Other recent investigations have also indicated the potential benefits of using VGs of various shapes with laminar flow at different Reynolds numbers [35,43,82].

- Indeed, developments in manufacturing capabilities and processes have opened wide possibilities for modifying the heat sink types to enhance the performance of cooling systems. Therefore, the air as a working fluid becomes limited to use in high heat flux devices. Now, an interesting question is: can perforated PHS be used with water to meet the requirement of electronics devises? Al-Asadi et al. [1] have answered this question. The perforated PHS cannot be used with water to enhance the heat transfer due to the difference of the thermo-physical properties between the air and water. Therefore, Al-Asadi et al. [1] have offered a new design of a uniform micro-channel with vortex generators (VGs) with different shapes and developed their investigation by using quarter and half-circle VGs [104]. They then developed the VG configurations to reduce the thermal resistance and pressure penalty by having a gap in the half-circle VGs [8]. Thus, the motivation of this sequence is to develop a design to enhance the heat transfer and reduce the power consumption of a micro cooling system.

Finally, the growing interest in the micro-channel heat sinks with VGs, which is evident by the number of available studies, leads to the conclusion that research in this fascinating area is still progressing and in need to further exploration. Moreover, there is a gap in knowledge on using micro-channels with liquid coolants (applications demand the capability to handle high heat-flux; therefore, developing liquid cooling systems is increasingly important).

Therefore, more studies are needed to investigate the common air-based heat sink with water as a working fluid [1]. Before presenting the investigation, it is important to illustrate the methodology of using temperature-independent Equations (9)–(12) [8].

Practically, especially for large heat flux conditions, an ionic liquid could be suggested [229] to enhance the heat transfer rate.

References

1.   Al-Asadi, M.; Al-Damook, A.; Wilson, M. Assessment of vortex generator shapes and pin fin perforations for enhancing water-based heat sink performance. *Int. Commun. Heat Mass Transf.* **2018**, *91*, 1–10. [CrossRef]
2.   Ahmed, H.; Mohammed, H.; Yusoff, M. An overview on heat transfer augmentation using vortex generators and nanofluids: Approaches and applications. *Renew. Sustain. Energy Rev.* **2012**, *16*, 5951–5993.
3.   Knight, R.W.; Goodling, J.S.; Hall, D.J. Optimal Thermal Design of Forced Convection Heat Sinks-Analytical. *J. Electron. Packag.* **1991**, *113*, 313–321. [CrossRef]
4.   Knight, R.; Goodling, J.; Gross, B. Optimal thermal design of air cooled forced convection finned heat sinks-experimental verification. In *IEEE Transactions on Components, Hybrids, and Manufacturing Technology*; IEEE: New York, NY, USA, 1992; pp. 754–760.
5.   Teertstra, P.; Yovanovich, M.M.; Culham, J.R. Analytical forced convection modeling of plate-fin heat sinks. *J. Electron. Manuf.* **2000**, *10*, 253–261. [CrossRef]
6.   Copeland, D. Optimization of parallel plate heatsinks for forced convection. In Proceedings of the Sixteenth Annual IEEE Semiconductor Thermal Measurement and Management Symposium, San Jose, CA, USA, 23 March 2000.
7.   Sparrow, E.M.; Ramsey, J.W.; Altemani, C.A.C. Experiments on In-line Pin Fin Arrays and Performance Comparisons with Staggered Arrays. *J. Heat Transf.* **1980**, *102*, 44–50. [CrossRef]
8.   Al-Asadi, M.T.; Alkasmoul, F.S.; Wilson, M.C. Benefits of spanwise gaps in cylindrical vortex generators for conjugate heat transfer enhancement in micro-channels. *Appl. Therm. Eng.* **2018**, *130*, 571–586. [CrossRef]
9.   Zhou, F.; Catton, I. Numerical Evaluation of Flow and Heat Transfer in Plate-Pin Fin Heat Sinks with Various Pin Cross-Sections. *Numer. Heat Transfer, Part A: Appl.* **2011**, *60*, 107–128. [CrossRef]
10. Jacobs, E.N. *Tests of Six Symmetrical Airfoils in the Variable Density Wind Tunnel*; NACA: Moffett Field, CA, USA, 1931.
11. Jacobs, E.N.; Ward, K.E.; Pinkerton, R.M. *The Characteristics of 78 Related Airfoil Sections from Tests in the Variable-Density Wind Tunnel*; NACA: Moffett Field, CA, USA, 1933; pp. 299–354.
12. Albadr, J.; Tayal, S.; Al-Asadi, M. Heat transfer through heat exchanger using Al_2O_3 nanofluid at different concentrations. *Case Stud. Therm. Eng.* **2013**, *1*, 38–44. [CrossRef]
13. Kherbeet, A.; Safaei, M.R.; Mohammed, H.A.; Salman, B.; Ahmed, H.; Alawi, O.A.; Al-Asadi, M. Heat transfer and fluid flow over microscale backward and forward facing step: A review. *Int. Commun. Heat Mass Transf.* **2016**, *76*, 237–244. [CrossRef]
14. Al-Asadi, M.; Mohammed, H.; Kherbeet, A.; Al-Aswadi, A. Numerical study of assisting and opposing mixed convective nanofluid flows in an inclined circular pipe. *Int. Commun. Heat Mass Transf.* **2017**, *85*, 81–91. [CrossRef]
15. Kherbeet, A.S.; Mohammed, H.; Ahmed, H.E.; Salman, B.; Alawi, O.A.; Safaei, M.R.; Khazaal, M. Mixed convection nanofluid flow over microscale forward-facing step—Effect of inclination and step heights. *Int. Commun. Heat Mass Transf.* **2016**, *78*, 145–154. [CrossRef]
16. Wang, C.-C.; Lo, J.; Lin, Y.-T.; Liu, M.-S. Flow visualization of wave-type vortex generators having inline fin-tube arrangement. *Int. J. Heat Mass Transf.* **2002**, *45*, 1933–1944. [CrossRef]
17. Depaiwa, N.; Chompookham, T.; Promvonge, P. Thermal enhancement in a solar air heater channel using rectangular winglet vortex generators. In Proceedings of the Proceedings of the International Conference on Energy and Sustainable Development: Issues and Strategies (ESD 2010), Chiang Mai, Thailand, 2–4 June 2010.
18. Li, H.-Y.; Chen, C.-L.; Chao, S.-M.; Liang, G.-F. Enhancing heat transfer in a plate-fin heat sink using delta winglet vortex generators. *Int. J. Heat Mass Transf.* **2013**, *67*, 666–677. [CrossRef]
19. Al-Asadi, M.T.; Mohammed, H.A.; Akhtar, S.N.; Kherbeet, A.S.; Dawood, H.K. Heat Transfer Enhancements Using Traditional Fluids and Nanofluids in Pipes with Different Orientations: A Review. *J. Nanofluids* **2017**, *6*, 987–1007. [CrossRef]

20. Soudagar, M.E.M.; Kalam, M.A.; Sajid, M.U.; Afzal, A.; Banapurmath, N.R.; Akram, N.; Mane, S.; C, A.S. Thermal analyses of minichannels and use of mathematical and numerical models. *Numer. Heat Transf. Part A Appl.* **2020**, *77*, 497–537. [CrossRef]

21. Ali, M.S.; Anwar, Z.; Mujtaba, M.; Soudagar, M.E.M.; Badruddin, I.A.; Safaei, M.R.; Iqbal, A.; Afzal, A.; Razzaq, L.; Khidmatgar, A.; et al. Two-phase frictional pressure drop with pure refrigerants in vertical mini/micro-channels. *Case Stud. Therm. Eng.* **2021**, *23*, 100824. [CrossRef]

22. Malakar, A.; Kanel, S.R.; Ray, C.; Snow, D.D.; Nadagouda, M.N. Nanomaterials in the environment, human exposure pathway, and health effects: A review. *Sci. Total Environ.* **2020**, *759*, 143470. [CrossRef]

23. Soudagar, M.E.M.; Nik-Ghazali, N.-N.; Kalam, A.; Badruddin, I.; Banapurmath, N.; Akram, N. The effect of nano-additives in diesel-biodiesel fuel blends: A comprehensive review on stability, engine performance and emission characteristics. *Energy Convers. Manag.* **2018**, *178*, 146–177. [CrossRef]

24. Ahmed, W.; Amin, M.; Ahmed, K.; Mehamood, S.; Fayaz, H.; Mujtaba, M.A.; Soudagar, M.E.M.; Gul, M. Characteristics investigation of silicone rubber-based RTV/µATH@nSiO$_2$ micro/nano composites for outdoor high voltage insulation. *J. Dispers. Sci. Technol.* **2021**, 1–14. [CrossRef]

25. Tuckerman, D.; Pease, R. High-performance heat sinking for VLSI. *IEEE Electron Device Lett.* **1981**, *2*, 126–129. [CrossRef]

26. Baghban, A.; Sasanipour, J.; Pourfayaz, F.; Ahmadi, M.H.; Kasaeian, A.; Chamkha, A.J.; Oztop, H.F.; Chau, K.-W. Towards experimental and modeling study of heat transfer performance of water- SiO2 nanofluid in quadrangular cross-section channels. *Eng. Appl. Comput. Fluid Mech.* **2019**, *13*, 453–469. [CrossRef]

27. Nagarani, N.; Mayilsamy, K.; Murugesan, A.; Kumar, G.S. Review of utilization of extended surfaces in heat transfer problems. *Renew. Sustain. Energy Rev.* **2014**, *29*, 604–613. [CrossRef]

28. Ahmed, S.C.; Asif, A.; Irfan, A.B.; Khan, T.M.Y.; Kamangar, S.; Abdelmohimen, M.; Soudagar, M.E.M.; Fayaz, H. Numerical investigation on pressure-driven electro osmatic flow and mixing in a constricted micro channel by triangular obstacle. *International J. Numer. Methods Heat Fluid Flow* **2021**, *31*, 982–1013.

29. Manca, O.; Nardini, S.; Ricci, D. A numerical study of nanofluid forced convection in ribbed channels. *Appl. Therm. Eng.* **2012**, *37*, 280–292. [CrossRef]

30. Ahmed, M.; Yusoff, M.; Ng, K.C.; Shuaib, N. Effect of corrugation profile on the thermal–hydraulic performance of corrugated channels using CuO–water nanofluid. *Case Stud. Therm. Eng.* **2014**, *4*, 65–75. [CrossRef]

31. Wang, C.-C.; Liaw, J.-S. Air-side performance of herringbone wavy fin-and-tube heat exchangers under dehumidifying condition – Data with larger diameter tube. *Int. J. Heat Mass Transf.* **2012**, *55*, 3054–3060. [CrossRef]

32. Li, L.; Du, X.; Zhang, Y.; Yang, L.; Yang, Y. Numerical simulation on flow and heat transfer of fin-and-tube heat exchanger with longitudinal vortex generators. *Int. J. Therm. Sci.* **2015**, *92*, 85–96. [CrossRef]

33. Johnson, T.R.; Joubert, P.N. The Influence of Vortex Generators on the Drag and Heat Transfer from a Circular Cylinder Normal to an Airstream. *J. Heat Transf.* **1969**, *91*, 91–99. [CrossRef]

34. Min, C.; Qi, C.; Kong, X.; Dong, J. Experimental study of rectangular channel with modified rectangular longitudinal vortex generators. *Int. J. Heat Mass Transf.* **2010**, *53*, 3023–3029. [CrossRef]

35. Chen, C.; Teng, J.-T.; Cheng, C.-H.; Jin, S.; Huang, S.; Liu, C.; Lee, M.-T.; Pan, H.-H.; Greif, R. A study on fluid flow and heat transfer in rectangular microchannels with various longitudinal vortex generators. *Int. J. Heat Mass Transf.* **2014**, *69*, 203–214. [CrossRef]

36. Ebrahimi, A.; Roohi, E.; Kheradmand, S. Numerical study of liquid flow and heat transfer in rectangular microchannel with longitudinal vortex generators. *Appl. Therm. Eng.* **2015**, *78*, 576–583.

37. Leu, J.-S.; Wu, Y.-H.; Jang, J.-Y. Heat transfer and fluid flow analysis in plate-fin and tube heat exchangers with a pair of block shape vortex generators. *Int. J. Heat Mass Transf.* **2004**, *47*, 4327–4338. [CrossRef]

38. Wu, J.; Tao, W. Effect of longitudinal vortex generator on heat transfer in rectangular channels. *Appl. Therm. Eng.* **2012**, *37*, 67–72.

39. Khoshvaght-Aliabadi, M.; Zangouei, S.; Hormozi, F. Performance of a plate-fin heat exchanger with vortex-generator channels: 3D-CFD simulation and experimental validation. *Int. J. Therm. Sci.* **2015**, *88*, 180–192.

40. Li, J.; Wang, S.; Chen, J.; Lei, Y.-G. Numerical study on a slit fin-and-tube heat exchanger with longitudinal vortex generators. *Int. J. Heat Mass Transf.* **2011**, *54*, 1743–1751.

41. Yang, K.-S.; Jhong, J.-H.; Lin, Y.-T.; Chien, K.-H.; Wang, C.-C. On the Heat Transfer Characteristics of Heat Sinks: With and Without Vortex Generators. *IEEE Trans. Components Packag. Technol.* **2010**, *33*, 391–397.

42. Chomdee, S.; Kiatsiriroat, T. Enhancement of air cooling in staggered array of electronic modules by integrating delta winglet vortex generators. *Int. Commun. Heat Mass Transf.* **2006**, *33*, 618–626. [CrossRef]

43. Liu, C.; Teng, J.-T.; Chu, J.-C.; Chiu, Y.-L.; Huang, S.; Jin, S.; Dang, T.; Greif, R.; Pan, H.-H. Experimental investigations on liquid flow and heat transfer in rectangular microchannel with longitudinal vortex generators. *Int. J. Heat Mass Transf.* **2011**, *54*, 3069–3080.

44. Ma, J.; Huang, Y.P.; Huang, J.; Wang, Y.L.; Wang, Q.W. Experimental investigations on single-phase heat transfer enhancement with longitudinal vortices in narrow rectangular channel. *Nucl. Eng. Des.* **2010**, *240*, 92–102.

45. Cheraghi, M.; Raisee, M.; Moghaddami, M. Effect of cylinder proximity to the wall on channel flow heat transfer enhancement. *C. R. Mécanique* **2014**, *342*, 63–72.

46. Safaei, M.R.; Jahanbin, A.; Kianifar, A.; Gharehkhani, S.; Kherbeet, A.S.; Goodarzi, M.; Dahari, M. *Mathematical Modeling for Nanofluids Simulation: A Review of the Latest Works, in Modeling and Simulation in Engineering Sciences*; Akbar, N.S., Beg, O.A., Eds.; InTechOpen: London, UK, 2016.

47. Koşar, A. Effect of substrate thickness and material on heat transfer in microchannel heat sinks. *Int. J. Therm. Sci.* **2010**, *49*, 635–642. [CrossRef]

48. Dixit, T.; Ghosh, I. Review of micro- and mini-channel heat sinks and heat exchangers for single phase fluids. *Renew. Sustain. Energy Rev.* **2015**, *41*, 1298–1311.

49. Mehendale, S.S.; Jacobi, A.; Shah, R.K. Fluid Flow and Heat Transfer at Micro- and Meso-Scales with Application to Heat Exchanger Design. *Appl. Mech. Rev.* **2000**, *53*, 175–193.

50. Kandlikar, S.G.; Grande, W.J. Evolution of microchannel flow passages: Thermohydraulic performance and fabrication technology. In Proceedings of the ASME International Mechanical Engineering Congress Exposition, New Orleans, LA, USA, 17–22 November 2002.

51. Abed, W.M.; Whalley, R.; Dennis, D.; Poole, R.J. Numerical and experimental investigation of heat transfer and fluid flow characteristics in a micro-scale serpentine channel. *Int. J. Heat Mass Transf.* **2015**, *88*, 790–802.

52. Choi, S.U.S.; Eastman, J.A. Enhancing thermal conductivity of fluids with nanoparticles. In Proceedings of the ASME International Mechanical Engineering Congress and Exposition, San Francisco, CA, USA, 12–17 November 1995. 8p.

53. Afzal, A.; Abidi, A.; Ad, M.; Rk, A.; Soudagar, M.E.M.; Saleel, A.C. Effect of parameters on thermal and fluid-flow behavior of battery thermal management system. *Therm. Sci.* **2021**, *25*, 3775–3787.

54. Fayaz, H.; Afzal, A.; Samee, A.D.M.; Soudagar, M.E.M.; Akram, N.; Mujtaba, M.A.; Jilte, R.D.; Islam, T.; Ağbulut, Ü.; Saleel, C.A. Optimization of Thermal and Structural Design in Lithium-Ion Batteries to Obtain Energy Efficient Battery Thermal Management System (BTMS): A Critical Review. *Arch. Comput. Methods Eng.* **2021**, *29*, 129–194.

55. Belkhode, P.N.; Shelare, S.D.; Sakhale, C.N.; Kumar, R.; Shanmugan, S.; Soudagar, M.E.M.; Mujtaba, M. Performance analysis of roof collector used in the solar updraft tower. *Sustain. Energy Technol. Assessments* **2021**, *48*, 101619.

56. Al Qubeissi, M.; Almshahy, A.; Mahmoud, A.; Al-Asadi, M.T.; Shah, R.M.R.A. Modelling of battery thermal management: A new concept of cooling using fuel. *Fuel* **2021**, *310*, 122403.

57. Shkarah, A.J.; Bin Sulaiman, M.Y.; Ayob, R.B.H.; Togun, H. A 3D numerical study of heat transfer in a single-phase micro-channel heat sink using graphene, aluminum and silicon as substrates. *Int. Commun. Heat Mass Transf.* **2013**, *48*, 108–115.

58. Lee, P.; Garimella, S.V. Thermally developing flow and heat transfer in rectangular microchannels of different aspect ratios. *Int. J. Heat Mass Transf.* **2006**, *49*, 3060–3067.

59. Mansoor, M.M.; Wong, K.C.; Siddique, M. Numerical investigation of fluid flow and heat transfer under high heat flux using rectangular micro-channels. *Int. Commun. Heat Mass Transf.* **2012**, *39*, 291–297. [CrossRef]

60. Lee, P.; Garimella, S.V.; Liu, D. Investigation of heat transfer in rectangular microchannels. *Int. J. Heat Mass Transf.* **2005**, *48*, 1688–1704. [CrossRef]

61. Deng, D.; Wan, W.; Tang, Y.; Wan, Z.; Liang, D. Experimental investigations on flow boiling performance of reentrant and rectangular microchannels – A comparative study. *Int. J. Heat Mass Transf.* **2015**, *82*, 435–446. [CrossRef]

62. Balaj, M.; Roohi, E.; Akhlaghi, H. Effects of shear work on non-equilibrium heat transfer characteristics of rarefied gas flows through micro/nanochannels. *Int. J. Heat Mass Transf.* **2015**, *83*, 69–74. [CrossRef]

63. Xia, G.; Jiang, J.; Wang, J.; Zhai, Y.; Ma, D. Effects of different geometric structures on fluid flow and heat transfer performance in microchannel heat sinks. *Int. J. Heat Mass Transf.* **2015**, *80*, 439–447. [CrossRef]

64. Ghasemian, M.; Ashrafi, Z.N.; Goharkhah, M.; Ashjaee, M. Heat transfer characteristics of Fe_3O_4 ferrofluid flowing in a mini channel under constant and alternating magnetic fields. *J. Magn. Magn. Mater.* **2015**, *381*, 158–167. [CrossRef]

65. Pongsoi, P.; Pikulkajorn, S.; Wongwises, S. Heat transfer and flow characteristics of spiral fin-and-tube heat exchangers: A review. *Int. J. Heat Mass Transf.* **2014**, *79*, 417–431. [CrossRef]

66. Pan, M.; Tang, Y.; Pan, L.; Lu, L. Optimal design of complex manifold geometries for uniform flow distribution between microchannels. *Chem. Eng. J.* **2008**, *137*, 339–346. [CrossRef]

67. Gamrat, G.; Favre-Marinet, M.; Asendrych, D. Conduction and entrance effects on laminar liquid flow and heat transfer in rectangular microchannels. *Int. J. Heat Mass Transf.* **2005**, *48*, 2943–2954. [CrossRef]

68. Qu, W.; Mudawar, I. Experimental and numerical study of pressure drop and heat transfer in a single-phase micro-channel heat sink. *Int. J. Heat Mass Transf.* **2002**, *45*, 2549–2565. [CrossRef]

69. Hsu, L.-C.; Cion, S.-W.; Lin, K.-W.; Wang, C.-C. An experimental study of inclination on the boiling heat transfer characteristics of a micro-channel heat sink using HFE-7100. *Int. Commun. Heat Mass Transf.* **2015**, *62*, 13–17. [CrossRef]

70. Suwankamnerd, P.; Wongwises, S. An experimental study of two-phase air–water flow and heat transfer characteristics of segmented flow in a microchannel. *Exp. Therm. Fluid Sci.* **2015**, *62*, 29–39. [CrossRef]

71. Mirmanto, M. Heat transfer coefficient calculated using a linear pressure gradient assumption and measurement for flow boiling in microchannels. *Int. J. Heat Mass Transf.* **2014**, *79*, 269–278. [CrossRef]

72. Konishi, C.; Lee, H.; Mudawar, I.; Hasan, M.M.; Nahra, H.K.; Hall, N.R.; Wagner, J.D.; May, R.L.; Mackey, J.R. Flow boiling in microgravity: Part 1—Interfacial behavior and experimental heat transfer results. *Int. J. Heat Mass Transf.* **2015**, *81*, 705–720. [CrossRef]

73. Gan, Y.; Xu, J.; Yan, Y. An experimental study of two-phase pressure drop of acetone in triangular silicon micro-channels. *Appl. Therm. Eng.* **2015**, *80*, 76–86. [CrossRef]

74. Fang, X.; Zhou, Z.; Wang, H. Heat transfer correlation for saturated flow boiling of water. *Appl. Therm. Eng.* **2015**, *76*, 147–156. [CrossRef]

75. Shojaeian, M.; Koşar, A. Pool boiling and flow boiling on micro- and nanostructured surfaces. *Exp. Therm. Fluid Sci.* **2015**, *63*, 45–73. [CrossRef]

76. Asadi, M.; Xie, G.; Sunden, B. A review of heat transfer and pressure drop characteristics of single and two-phase microchannels. *Int. J. Heat Mass Transf.* **2014**, *79*, 34–53. [CrossRef]

77. Analytics Clarivate. *Acquisition of the Thomson Reuters Intellectual Property and Science web of Science*; Clarivate: London, UK, 2017.

78. Guo, J.; Xu, M.; Cheng, L. Numerical investigations of curved square channel from the viewpoint of field synergy principle. *Int. J. Heat Mass Transf.* **2011**, *54*, 4148–4151. [CrossRef]

79. Chu, J.-C.; Teng, J.-T.; Greif, R. Experimental and numerical study on the flow characteristics in curved rectangular microchannels. *Appl. Therm. Eng.* **2010**, *30*, 1558–1566. [CrossRef]

80. Dehghan, M.; Daneshipour, M.; Valipour, M.S.; Rafee, R.; Saedodin, S. Enhancing heat transfer in microchannel heat sinks using converging flow passages. *Energy Convers. Manag.* **2015**, *92*, 244–250. [CrossRef]

81. Aris, M.; Owen, I.; Sutcliffe, C. The development of active vortex generators from shape memory alloys for the convective cooling of heated surfaces. *Int. J. Heat Mass Transf.* **2011**, *54*, 3566–3574. [CrossRef]

82. Mirzaee, H.; Dadvand, A.; Mirzaee, I.; Shabani, R. Heat transfer enhancement in microchannels using an elastic vortex generator. *J. Enhanc. Heat Transf.* **2012**, *19*, 199–211. [CrossRef]

83. Liu, J.; Xie, G.; Simon, T.W. Turbulent flow and heat transfer enhancement in rectangular channels with novel cylindrical grooves. *Int. J. Heat Mass Transf.* **2015**, *81*, 563–577. [CrossRef]

84. Bi, C.; Tang, G.; Tao, W. Heat transfer enhancement in mini-channel heat sinks with dimples and cylindrical grooves. *Appl. Therm. Eng.* **2013**, *55*, 121–132. [CrossRef]

85. Zhai, Y.; Xia, G.; Liu, X.; Li, Y. Exergy analysis and performance evaluation of flow and heat transfer in different micro heat sinks with complex structure. *Int. J. Heat Mass Transf.* **2015**, *84*, 293–303. [CrossRef]

86. Knupp, D.; Cotta, R.; Naveira-Cotta, C.P. Fluid flow and conjugated heat transfer in arbitrarily shaped channels via single domain formulation and integral transforms. *Int. J. Heat Mass Transf.* **2015**, *82*, 479–489. [CrossRef]

87. Henze, M.; von Wolfersdorf, J. Influence of approach flow conditions on heat transfer behind vortex generators. *Int. J. Heat Mass Transf.* **2011**, *54*, 279–287. [CrossRef]

88. Dai, Z.; Fletcher, D.F.; Haynes, B.S. Impact of tortuous geometry on laminar flow heat transfer in microchannels. *Int. J. Heat Mass Transf.* **2015**, *83*, 382–398. [CrossRef]

89. Karathanassis, I.; Papanicolaou, E.; Belessiotis, V.; Bergeles, G. Experimental and numerical evaluation of an elongated plate-fin heat sink with three sections of stepwise varying channel width. *Int. J. Heat Mass Transf.* **2015**, *84*, 16–34. [CrossRef]

90. Kundu, B.; Das, P.K. Performance and optimum design analysis of convective fin arrays attached to flat and curved primary surfaces. *Int. J. Refrig.* **2009**, *32*, 430–443. [CrossRef]

91. Hong, F.; Cheng, P.; Ge, H.; Joo, G.T. Conjugate heat transfer in fractal-shaped microchannel network heat sink for integrated microelectronic cooling application. *Int. J. Heat Mass Transf.* **2007**, *50*, 4986–4998. [CrossRef]

92. Torii, K.; Kwak, K.; Nishino, K. Heat transfer enhancement accompanying pressure-loss reduction with winglet-type vortex generators for fin-tube heat exchangers. *Int. J. Heat Mass Transf.* **2002**, *45*, 3795–3801. [CrossRef]

93. Zhang, Y.H.; Wang, L.B.; Ke, F.; Su, Y.X.; Gao, S.D. The effects of span position of winglet vortex generator on local heat/mass transfer over a three-row flat tube bank fin. *Heat Mass Transf.* **2004**, *40*, 881–891. [CrossRef]

94. Wang, C.-C.; Lo, J.; Lin, Y.-T.; Wei, C.-S. Flow visualization of annular and delta winlet vortex generators in fin-and-tube heat exchanger application. *Int. J. Heat Mass Transf.* **2002**, *45*, 3803–3815. [CrossRef]

95. Ahmed, S.; Mohammed, W.; Laith, J. Numerical investigation into velocity and temperature fields over smooth and rough ducts for several types of turbulators. *J. Eng. Technol.* **2007**, *25*, 1110–1128.

96. Gorji-Bandpy, M.; Soleimani, S.; Hossein-Nejad, F. Pressure and Heat Transfer in Staggered Arrangement Circular Tubes with Airfoil Vortex Generator. *Int. Energy J.* **2008**, *9*, 207–214.

97. Wang, J.; Zhao, Y. Heat and fluid flow characteristics of a rectangular channel with a small diameter circular cylinder as vortex generator. *Int. J. Therm. Sci.* **2015**, *92*, 1–13. [CrossRef]

98. Chai, L.; Xia, G.; Wang, H.S. Numerical study of laminar flow and heat transfer in microchannel heat sink with offset ribs on sidewalls. *Appl. Therm. Eng.* **2016**, *92*, 32–41. [CrossRef]

99. Chai, L.; Xia, G.D.; Wang, H. Parametric study on thermal and hydraulic characteristics of laminar flow in microchannel heat sink with fan-shaped ribs on sidewalls—Part 1: Heat transfer. *Int. J. Heat Mass Transf.* **2016**, *97*, 1069–1080. [CrossRef]

100. Chai, L.; Xia, G.D.; Wang, H. Parametric study on thermal and hydraulic characteristics of laminar flow in microchannel heat sink with fan-shaped ribs on sidewalls—Part 2: Pressure drop. *Int. J. Heat Mass Transf.* **2016**, *97*, 1081–1090. [CrossRef]

101. Chai, L.; Xia, G.D.; Wang, H. Parametric study on thermal and hydraulic characteristics of laminar flow in microchannel heat sink with fan-shaped ribs on sidewalls – Part 3: Performance evaluation. *Int. J. Heat Mass Transf.* **2016**, *97*, 1091–1101. [CrossRef]

102. Li, Y.; Xia, G.; Ma, D.; Jia, Y.; Wang, J. Characteristics of laminar flow and heat transfer in microchannel heat sink with triangular cavities and rectangular ribs. *Int. J. Heat Mass Transf.* **2016**, *98*, 17–28. [CrossRef]

103. Behnampour, A.; Akbari, O.A.; Safaei, M.R.; Ghavami, M.; Marzban, A.; Shabani, G.A.S.; Zarringhalam, M.; Mashayekhi, R. Analysis of heat transfer and nanofluid fluid flow in microchannels with trapezoidal, rectangular and triangular shaped ribs. *Phys. E Low-Dimens. Syst. Nanostruct.* **2017**, *91*, 15–31. [CrossRef]

104. Al-Asadi, M.; Alkasmoul, F.; Wilson, M. Heat transfer enhancement in a micro-channel cooling system using cylindrical vortex generators. *Int. Commun. Heat Mass Transf.* **2016**, *74*, 40–47. [CrossRef]

105. Raihan, M.F.B.; Al-Asadi, M.T.; Thompson, H. Management of conjugate heat transfer using various arrangements of cylindrical vortex generators in micro-channels. *Appl. Therm. Eng.* **2021**, *182*, 116097. [CrossRef]

106. Jama, M.; Singh, T.; Gamaleldin, S.M.; Koc, M.; Samara, A.; Isaifan, R.; Atieh, M.A. Critical Review on Nanofluids: Preparation, Characterization, and Applications. *J. Nanomater.* **2016**, *2016*, 1–22. [CrossRef]

107. Li, Y.; Zhou, J.; Tung, S.; Schneider, E.; Xi, S. A review on development of nanofluid preparation and characterization. *Powder Technol.* **2009**, *196*, 89–101. [CrossRef]

108. Kakaç, S.; Pramuanjaroenkij, A. Single-phase and two-phase treatments of convective heat transfer enhancement with nanofluids— A state-of-the-art review. *Int. J. Therm. Sci.* **2016**, *100*, 75–97. [CrossRef]

109. Azmi, W.; Hamid, K.A.; Usri, N.; Mamat, R.; Sharma, K. Heat transfer augmentation of ethylene glycol: Water nanofluids and applications—A review. *Int. Commun. Heat Mass Transf.* **2016**, *75*, 13–23. [CrossRef]

110. Eastman, J.A.; Choi, U.S.; Li, S.; Thompson, L.J.; Lee, S. Enhanced Thermal Conductivity through the Development of Nanofluids. *MRS Proc.* **1996**, *457*, 3–11. [CrossRef]

111. Lee, S.; Choi, S.U.-S.; Li, S.; Eastman, J. Measuring Thermal Conductivity of Fluids Containing Oxide Nanoparticles. *J. Heat Transf.* **1999**, *121*, 280–289. [CrossRef]

112. Choi, S.U.S.; Eastman, J.A. *Enhanced Heat Transfer Using Nanofluids*; Argonne National Laboratory (ANL): Argonne, IL, USA, 2001.

113. Choi, S.U.S.; Zhang, Z.G.; Yu, W.; Lockwood, F.E.; Grulke, E.A. Anomalous thermal conductivity enhancement in nanotube suspensions. *Appl. Phys. Lett.* **2001**, *79*, 2252–2254. [CrossRef]

114. Zhu, H.-T.; Lin, Y.-S.; Yin, Y.-S. A novel one-step chemical method for preparation of copper nanofluids. *J. Colloid Interface Sci.* **2004**, *277*, 100–103. [CrossRef] [PubMed]

115. Gleiter, H. Nanocrystalline Materials. In *Advanced Structural and Functional Materials: Proceedings of an International Seminar Organized by Deutsche Forschungsanstalt für Luft- und Raumfahrt (DLR), Köln, June 1991*; Bunk, W.G.J., Ed.; Springer: Berlin/Heidelberg, Germany, 1991; pp. 1–37.

116. Ashley, S. Small-scale structure yields big property payoffs. *Mech. Eng.* **1994**, *116*, 52.

117. Bowles, R.; Kolstad, J.; Calo, J.; Andres, R. Generation of molecular clusters of controlled size. *Surf. Sci.* **1981**, *106*, 117–124. [CrossRef]

118. IIijima, S. Helical microtubules of graphitic carbon. *Nature* **1991**, *354*, 56–58. [CrossRef]

119. Menni, Y.; Chamkha, A.J.; Ghazvini, M.; Ahmadi, M.H.; Ameur, H.; Issakhov, A.; Inc, M. Enhancement of the turbulent convective heat transfer in channels through the baffling technique and oil/multiwalled carbon nanotube nanofluids. *Numer. Heat Transfer, Part A Appl.* **2021**, *79*, 311–351. [CrossRef]

120. Scott, C.; Arepalli, S.; Nikolaev, P.; Smalley, R. Growth mechanisms for single-wall carbon nanotubes in a laser-ablation process. *Appl. Phys. A* **2001**, *72*, 573–580. [CrossRef]

121. Hernadi, K. Catalytic synthesis of multiwall carbon nanotubes from methylacetylene. *Chem. Phys. Lett.* **2002**, *363*, 169–174. [CrossRef]

122. Yatsuya, S.; Tsukasaki, Y.; Mihama, K.; Uyeda, R. Preparation of extremely fine particles by vacuum evaporation onto a running oil substrate. *J. Cryst. Growth* **1978**, *45*, 490–494. [CrossRef]

123. Eastman, J.A. *Novel Applications Exploiting the Thermal Properties of Nanostructured Materials. ANL/MSD/CP-97456*; Argonne National Lab: Argone, IL, USA, 1998.

124. Mohammed, H.A.; Bhaskaran, G.; Shuaib, N.; Saidur, R. Heat transfer and fluid flow characteristics in microchannels heat exchanger using nanofluids: A review. *Renew. Sustain. Energy Rev.* **2011**, *15*, 1502–1512. [CrossRef]

125. Rayleigh, L. LVI. On the influence of obstacles arranged in rectangular order upon the properties of a medium. *London Edinburgh Dublin Philos. Mag. J. Sci.* **1892**, *34*, 481–502. [CrossRef]

126. Fricke, H. A Mathematical Treatment of the Electric Conductivity and Capacity of Disperse Systems I. The Electric Conductivity of a Suspension of Homogeneous Spheroids. *Phys. Rev.* **1924**, *24*, 575–587. [CrossRef]

127. Fricke, H. The Maxwell-Wagner dispersion in a suspension of ellipsoids. *J. Phys. Chem.* **1953**, *57*, 934–937. [CrossRef]

128. Böttcher, C. The dielectric constant of crystalline powders. *Recl. Trav. Chim. Pays-Bas* **1945**, *64*, 47–51. [CrossRef]

129. Landauer, R. The electrical resistance of binary metallic mixtures. *J. Appl. Phys.* **1952**, *23*, 779–784. [CrossRef]

130. Jeffrey, D. Conduction through a random suspension of spheres. *Proc. R. Soc. London. Ser. A, Math. Phys. Sci.* **1973**, *335*, 355–367.

131. Davis, R. The effective thermal conductivity of a composite material with spherical inclusions. *Int. J. Thermophys.* **1986**, *7*, 609–620. [CrossRef]

132. Nan, C.-W.; Birringer, R.; Clarke, D.; Gleiter, H. Effective thermal conductivity of particulate composites with interfacial thermal resistance. *J. Appl. Phys.* **1997**, *81*, 6692–6699. [CrossRef]

133. Lu, S.-Y.; Song, J.-L. Effective conductivity of composites with spherical inclusions: Effect of coating and detachment. *J. Appl. Phys.* **1996**, *79*, 609–618. [CrossRef]

134. Benveniste, Y. Effective thermal conductivity of composites with a thermal contact resistance between the constituents: Nondilute case. *J. Appl. Phys.* **1987**, *61*, 2840–2843. [CrossRef]

135. Hasselman, D.P.H.; Johnson, L.F. Effective Thermal Conductivity of Composites with Interfacial Thermal Barrier Resistance. *J. Compos. Mater.* **1987**, *21*, 508–515. [CrossRef]

136. Abed, A.M.; Sopian, K.; Mohammed, H.; Alghoul, M.; Ruslan, M.H.; Mat, S.; Al-Shamani, A.N. Enhance heat transfer in the channel with V-shaped wavy lower plate using liquid nanofluids. *Case Stud. Therm. Eng.* **2015**, *5*, 13–23. [CrossRef]

137. Wang, X.; Xu, X.; Choi, S.U.S. Thermal Conductivity of Nanoparticle - Fluid Mixture. *J. Thermophys. Heat Transf.* **1999**, *13*, 474–480. [CrossRef]

138. Das, S.K.; Putra, N.; Thiesen, P.H.; Roetzel, W. Temperature Dependence of Thermal Conductivity Enhancement for Nanofluids. *J. Heat Transf.* **2003**, *125*, 567–574. [CrossRef]

139. Xie, H.; Wang, J.; Xi, T.; Liu, Y.; Ai, F.; Wu, Q. Thermal conductivity enhancement of suspensions containing nanosized alumina particles. *J. Appl. Phys.* **2002**, *91*, 4568–4572. [CrossRef]

140. Li, C.H.; Peterson, G.P. Experimental investigation of temperature and volume fraction variations on the effective thermal conductivity of nanoparticle suspensions (nanofluids). *J. Appl. Phys.* **2006**, *99*, 084314. [CrossRef]

141. Wen, D.; Ding, Y. Experimental investigation into convective heat transfer of nanofluids at the entrance region under laminar flow conditions. *Int. J. Heat Mass Transf.* **2004**, *47*, 5181–5188. [CrossRef]

142. Yoo, D.-H.; Hong, K.; Yang, H.-S. Study of thermal conductivity of nanofluids for the application of heat transfer fluids. *Thermochim. Acta* **2007**, *455*, 66–69. [CrossRef]

143. Zhang, X.; Gu, H.; Fujii, M. Experimental Study on the Effective Thermal Conductivity and Thermal Diffusivity of Nanofluids. *Int. J. Thermophys.* **2006**, *27*, 569–580. [CrossRef]

144. Kim, S.; Bang, I.; Buongiorno, J.; Hu, L. Surface wettability change during pool boiling of nanofluids and its effect on critical heat flux. *Int. J. Heat Mass Transf.* **2007**, *50*, 4105–4116. [CrossRef]

145. Li, C.H.; Peterson, G.P. The effect of particle size on the effective thermal conductivity of Al_2O_3-water nanofluids. *J. Appl. Phys.* **2007**, *101*, 44312. [CrossRef]

146. Beck, M.P.; Yuan, Y.; Warrier, P.; Teja, A.S. The effect of particle size on the thermal conductivity of alumina nanofluids. *J. Nanoparticle Res.* **2009**, *11*, 1129–1136. [CrossRef]

147. Mintsa, H.A.; Roy, G.; Nguyen, C.T.; Doucet, D. New temperature dependent thermal conductivity data for water-based nanofluids. *Int. J. Therm. Sci.* **2009**, *48*, 363–371. [CrossRef]

148. Jwo, C.-S.; Teng, T.-P.; Chang, H. A simple model to estimate thermal conductivity of fluid with acicular nanoparticles. *J. Alloy. Compd.* **2007**, *434–435*, 569–571. [CrossRef]

149. Murshed, S.M.S.; Leong, K.C.; Yang, C. Enhanced thermal conductivity of TiO_2—Water based nanofluids. *Int. J. Therm. Sci.* **2005**, *44*, 367–373. [CrossRef]

150. Wen, D.; Ding, Y. Natural convective heat transfer of suspensions of titanium dioxide nanoparticles (nanofluids). *IEEE Trans. Nanotechnol.* **2006**, *5*, 220–227.

151. He, Y.; Jin, Y.; Chen, H.; Ding, Y.; Cang, D.; Lu, H. Heat transfer and flow behaviour of aqueous suspensions of TiO_2 nanoparticles (nanofluids) flowing upward through a vertical pipe. *Int. J. Heat Mass Transf.* **2007**, *50*, 2272–2281. [CrossRef]

152. Turgut, A.; Tavman, I.; Chirtoc, M.; Schuchmann, H.P.; Sauter, C.; Tavman, S. Thermal Conductivity and Viscosity Measurements of Water-Based TiO_2 Nanofluids. *Int. J. Thermophys.* **2009**, *30*, 1213–1226. [CrossRef]

153. Zhu, H.; Zhang, C.; Liu, S.; Tang, Y.; Yin, Y. Effects of nanoparticle clustering and alignment on thermal conductivities of Fe_3O_4 aqueous nanofluids. *Appl. Phys. Lett.* **2006**, *89*, 023123. [CrossRef]

154. Hwang, Y.; Ahn, Y.; Shin, H.; Lee, C.; Kim, G.; Park, H.; Lee, J. Investigation on characteristics of thermal conductivity enhancement of nanofluids. *Curr. Appl. Phys.* **2006**, *6*, 1068–1071. [CrossRef]

155. Eastman, J.A.; Choi, S.U.S.; Li, S.; Yu, W.; Thompson, L.J. Anomalously increased effective thermal conductivities of ethylene glycol-based nanofluids containing copper nanoparticles. *Appl. Phys. Lett.* **2001**, *78*, 718–720. [CrossRef]

156. Xuan, Y.; Li, Q. Heat transfer enhancement of nanofluids. *Int. J. Heat Fluid Flow* **2000**, *21*, 58–64. [CrossRef]

157. Liu, M.-S.; Lin, M.C.-C.; Tsai, C.; Wang, C.-C. Enhancement of thermal conductivity with Cu for nanofluids using chemical reduction method. *Int. J. Heat Mass Transf.* **2006**, *49*, 3028–3033. [CrossRef]

158. Hong, T.-K.; Yang, H.-S.; Choi, C.J. Study of the enhanced thermal conductivity of Fe nanofluids. *J. Appl. Phys.* **2005**, *97*, 064311. [CrossRef]

159. Hong, K.S.; Hong, T.-K.; Yang, H.-S. Thermal conductivity of Fe nanofluids depending on the cluster size of nanoparticles. *Appl. Phys. Lett.* **2006**, *88*, 031901. [CrossRef]

160. Patel, H.E.; Das, S.K.; Sundararajan, T.; Nair, A.S.; George, B.; Pradeep, T. Thermal conductivities of naked and monolayer protected metal nanoparticle based nanofluids: Manifestation of anomalous enhancement and chemical effects. *Appl. Phys. Lett.* **2003**, *83*, 2931–2933. [CrossRef]

161. Putnam, S.A.; Cahill, D.G.; Braun, P.V.; Ge, Z.; Shimmin, R.G. Thermal conductivity of nanoparticle suspensions. *J. Appl. Phys.* **2006**, *99*, 084308. [CrossRef]

162. Heris, S.Z.; Esfahany, M.N.; Etemad, S. Experimental investigation of convective heat transfer of Al_2O_3/water nanofluid in circular tube. *Int. J. Heat Fluid Flow* **2007**, *28*, 203–210. [CrossRef]

163. Pak, B.C.; Cho, Y.I. Hydrodynamic and heat transfer study of dispersed fluids with submicron metallic oxide particles. *Exp. Heat Transf.* **1998**, *11*, 151–170. [CrossRef]

164. Hwang, K.S.; Jang, S.P.; Choi, S.U. Flow and convective heat transfer characteristics of water-based Al_2O_3 nanofluids in fully developed laminar flow regime. *Int. J. Heat Mass Transf.* **2009**, *52*, 193–199. [CrossRef]

165. Heris, S.Z.; Etemad, S.; Esfahany, M.N. Experimental investigation of oxide nanofluids laminar flow convective heat transfer. *Int. Commun. Heat Mass Transf.* **2006**, *33*, 529–535. [CrossRef]

166. Maxwell, J.C. *A Treatise on Electricity and Magnetism*; Clarendon: London, UK, 1892; Volume 1.

167. Bruggeman, D. Calculation of various physics constants in heterogenous substances I Dielectricity constants and conductivity of mixed bodies from isotropic substances. *Ann. Phys.* **1935**, *24*, 636–664. [CrossRef]

168. Yu, W.; Choi, S. The Role of Interfacial Layers in the Enhanced Thermal Conductivity of Nanofluids: A Renovated Maxwell Model. *J. Nanoparticle Res.* **2003**, *5*, 167–171. [CrossRef]

169. Xie, H.; Fujii, M.; Zhang, X. Effect of interfacial nanolayer on the effective thermal conductivity of nanoparticle-fluid mixture. *Int. J. Heat Mass Transf.* **2005**, *48*, 2926–2932. [CrossRef]

170. Shima, P.D.; Philip, J.; Raj, B. Role of microconvection induced by Brownian motion of nanoparticles in the enhanced thermal conductivity of stable nanofluids. *Appl. Phys. Lett.* **2009**, *94*, 223101. [CrossRef]

171. Vadasz, P. *Nano Uid Suspensions and Bi-Composite Media as Derivatives of interface Heat Transfer Modeling in Porous Media. Emerging Topics in Heat and Mass Transfer in Porous Media: From Bioengineering and Microelectronics to Nanotechnology*; Springer: Cham, Switzerland, 2008; 283p.

172. Prasher, R.; Phelan, P.E.; Bhattacharya, P. Effect of Aggregation Kinetics on the Thermal Conductivity of Nanoscale Colloidal Solutions (Nanofluid). *Nano Lett.* **2006**, *6*, 1529–1534. [CrossRef]

173. Nie, C.; Marlow, W.; Hassan, Y. Discussion of proposed mechanisms of thermal conductivity enhancement in nanofluids. *Int. J. Heat Mass Transf.* **2008**, *51*, 1342–1348. [CrossRef]

174. Ghasemi, B.; Aminossadati, S. Brownian motion of nanoparticles in a triangular enclosure with natural convection. *Int. J. Therm. Sci.* **2010**, *49*, 931–940. [CrossRef]

175. Xuan, Y.; Roetzel, W. Conceptions for heat transfer correlation of nanofluids. *Int. J. Heat Mass Transf.* **2000**, *43*, 3701–3707. [CrossRef]

176. Yu, W.; France, D.M.; Routbort, J.L.; Choi, S.U.S. Review and Comparison of Nanofluid Thermal Conductivity and Heat Transfer Enhancements. *Heat Transf. Eng.* **2008**, *29*, 432–460. [CrossRef]

177. Patel, H.E.; Sundararajan, T.; Das, S.K. An experimental investigation into the thermal conductivity enhancement in oxide and metallic nanofluids. *J. Nanoparticle Res.* **2010**, *12*, 1015–1031. [CrossRef]

178. Tillman, P.; Hill, J.M. Modelling the Thermal Conductivity of Nanofluids. In *IUTAM Symposium on Mechanical Behavior and Micro-Mechanics of Nanostructured Materials: Proceedings of the IUTAM Symposium, Beijing, China, 27–30 June 2005*; Bai, Y.L., Zheng, Q.S., Wei, Y.G., Eds.; Springer: Dordrecht, The Netherlands, 2007; pp. 105–118.

179. Xie, H.; Wang, J.; Xi, T.; Liu, Y.; Ai, F. Dependence of the thermal conductivity of nanoparticle-fluid mixture on the base fluid. *J. Mater. Sci. Lett.* **2002**, *21*, 1469–1471. [CrossRef]

180. Godson, L.; Raja, B.; Lal, D.M.; Wongwises, S. Enhancement of heat transfer using nanofluids—An overview. *Renew. Sustain. Energy Rev.* **2010**, *14*, 629–641. [CrossRef]

181. Sharma, P.; Baek, I.-H.; Cho, T.; Park, S.; Lee, K.B. Enhancement of thermal conductivity of ethylene glycol based silver nanofluids. *Powder Technol.* **2011**, *208*, 7–19. [CrossRef]

182. Madhusree, K.; Dey, T.K. Thermal conductivity and viscosity of Al_2O_3 nanofluid based on car engine coolant. *J. Phys. D Appl. Phys.* **2010**, *43*, 315501.

183. Corcione, M. Heat transfer features of buoyancy-driven nanofluids inside rectangular enclosures differentially heated at the sidewalls. *Int. J. Therm. Sci.* **2010**, *49*, 1536–1546. [CrossRef]

184. Al-Aswadi, A.; Mohammed, H.; Shuaib, N.; Campo, A. Laminar forced convection flow over a backward facing step using nanofluids. *Int. Commun. Heat Mass Transf.* **2010**, *37*, 950–957. [CrossRef]

185. Guo, S.-Z.; Li, Y.; Jiang, J.-S.; Xie, H.-Q. Nanofluids Containing γ-Fe2O3 Nanoparticles and Their Heat Transfer Enhancements. *Nanoscale Res. Lett.* **2010**, *5*, 1222–1227. [CrossRef]

186. Mohammed, H.; Al-Aswadi, A.; Shuaib, N.; Saidur, R. Convective heat transfer and fluid flow study over a step using nanofluids: A review. *Renew. Sustain. Energy Rev.* **2011**, *15*, 2921–2939. [CrossRef]

187. Yulong, D.; Chen, H.; Musina, Z.; Jin, Y.; Zhang, T.; Witharana, S.; Yang, W. Relationship between the thermal conductivity and shear viscosity of nanofluids. *Phys. Scr.* **2010**, *2010*, 014078.

188. Liu, M.-S.; Lin, M.C.-C.; Huang, I.-T.; Wang, C.-C. Enhancement of thermal conductivity with carbon nanotube for nanofluids. *Int. Commun. Heat Mass Transf.* **2005**, *32*, 1202–1210. [CrossRef]

189. Kumar, N.; Sonawane, S.S. Experimental study of thermal conductivity and convective heat transfer enhancement using CuO and TiO_2 nanoparticles. *Int. Commun. Heat Mass Transf.* **2016**, *76*, 98–107. [CrossRef]

190. Buongiorno, J.; Venerus, D.C.; Prabhat, N.; McKrell, T.J.; Townsend, J.; Christianson, R.J.; Tolmachev, Y.V.; Keblinski, P.; Hu, L.-W.; Alvarado, J.L.; et al. A benchmark study on the thermal conductivity of nanofluids. *J. Appl. Phys.* **2009**, *106*, 094312. [CrossRef]

191. Bigdeli, M.B.; Fasano, M.; Cardellini, A.; Chiavazzo, E.; Asinari, P. A review on the heat and mass transfer phenomena in nanofluid coolants with special focus on automotive applications. *Renew. Sustain. Energy Rev.* **2016**, *60*, 1615–1633. [CrossRef]

192. Das, S.K.; Choi, S.U.; Yu, W.; Pradeep, T. *Nanofluids: Science and Technology*; John Wiley & Sons: Hoboken, NJ, USA, 2007.

193. Krajnik, P.; Pusavec, F.; Rashid, A. Nanofluids: Properties, Applications and Sustainability Aspects in Materials Processing Technologies. In *Advances in Sustainable Manufacturing: Proceedings of the 8th Global Conference on Sustainable Manufacturing*; Seliger, G., Khraisheh, M.K.M., Jawahir, I.S., Eds.; Springer: Berlin/Heidelberg, Germany, 2011; pp. 107–113.

194. Colla, L.; Marinelli, L.; Fedele, L.; Bobbo, S.; Manca, O. Characterization and Simulation of the Heat Transfer Behaviour of Water-Based ZnO Nanofluids. *J. Nanosci. Nanotechnol.* **2015**, *15*, 3599–3609. [CrossRef]

195. Ahammed, N.; Asirvatham, G.; Titus, J.; Bose, J.R.; Wongwises, S. Measurement of thermal conductivity of graphene–water nanofluid at below and above ambient temperatures. *Int. Commun. Heat Mass Transf.* **2016**, *70*, 66–74. [CrossRef]

196. Kherbeet, A.; Mohammed, H.; Salman, B. The effect of nanofluids flow on mixed convection heat transfer over microscale backward-facing step. *Int. J. Heat Mass Transf.* **2012**, *55*, 5870–5881. [CrossRef]

197. Kherbeet, A.; Mohammed, H.; Salman, B.; Ahmed, H.E.; Alawi, O.A. Experimental and numerical study of nanofluid flow and heat transfer over microscale backward-facing step. *Int. J. Heat Mass Transf.* **2014**, *79*, 858–867. [CrossRef]

198. Salman, B.; Mohammed, H.A.; Kherbeet, A. Numerical and experimental investigation of heat transfer enhancement in a microtube using nanofluids. *Int. Commun. Heat Mass Transf.* **2014**, *59*, 88–100. [CrossRef]

199. Haridas, D.; Rajput, N.S.; Srivastava, A. Interferometric study of heat transfer characteristics of Al_2O_3 and SiO_2-based dilute nanofluids under simultaneously developing flow regime in compact channels. *Int. J. Heat Mass Transf.* **2015**, *88*, 713–727. [CrossRef]

200. Arighaleslami, A.H.; Walmsley, T.G.; Atkins, M.J.; Walmsley, M.R.; Neale, J.R. Heat Transfer Enhancement for site level indirect heat recovery systems using nanofluids as the intermediate fluid. *Appl. Therm. Eng.* **2016**, *105*, 923–930. [CrossRef]

201. Shahrul, I.; Mahbubul, I.; Saidur, R.; Sabri, M.F.M. Experimental investigation on Al_2O_3–W, SiO2–W and ZnO–W nanofluids and their application in a shell and tube heat exchanger. *Int. J. Heat Mass Transf.* **2016**, *97*, 547–558. [CrossRef]

202. Chon, C.H.; Kihm, K.D.; Lee, S.P.; Choi, S.U.S. Empirical correlation finding the role of temperature and particle size for nanofluid (Al_2O_3) thermal conductivity enhancement. *Appl. Phys. Lett.* **2005**, *87*, 153107. [CrossRef]

203. Keblinski, P.; Prasher, R.; Eapen, J. Thermal conductance of nanofluids: Is the controversy over? *J. Nanoparticle Res.* **2008**, *10*, 1089–1097. [CrossRef]

204. Behrangzade, A.; Heyhat, M.M. The effect of using nano-silver dispersed water based nanofluid as a passive method for energy efficiency enhancement in a plate heat exchanger. *Appl. Therm. Eng.* **2016**, *102*, 311–317. [CrossRef]

205. Salehi, J.M.; Heyhat, M.M.; Rajabpour, A. Enhancement of thermal conductivity of silver nanofluid synthesized by a one-step method with the effect of polyvinylpyrrolidone on thermal behavior. *Appl. Phys. Lett.* **2013**, *102*, 231907. [CrossRef]

206. Özerinç, S.; Kakaç, S.; Yazıcıoğlu, A.G. Enhanced thermal conductivity of nanofluids: A state-of-the-art review. *Microfluid. Nanofluidics* **2010**, *8*, 145–170. [CrossRef]

207. Lin, C.-Y.; Wang, J.-C.; Chen, T.-C. Analysis of suspension and heat transfer characteristics of Al_2O_3 nanofluids prepared through ultrasonic vibration. *Appl. Energy* **2011**, *88*, 4527–4533. [CrossRef]

208. Colangelo, G.; Favale, E.; de Risi, A.; Laforgia, D. Results of experimental investigations on the heat conductivity of nanofluids based on diathermic oil for high temperature applications. *Appl. Energy* **2012**, *97*, 828–833. [CrossRef]

209. Gupta, M.; Arora, N.; Kumar, R.; Kumar, S.; Dilbaghi, N. A comprehensive review of experimental investigations of forced convective heat transfer characteristics for various nanofluids. *Int. J. Mech. Mater. Eng.* **2014**, *9*, 1–21. [CrossRef]

210. Heyhat, M.; Kowsary, F.; Rashidi, A.; Momenpour, M.; Amrollahi, A. Experimental investigation of laminar convective heat transfer and pressure drop of water-based Al_2O_3 nanofluids in fully developed flow regime. *Exp. Therm. Fluid Sci.* **2013**, *44*, 483–489. [CrossRef]

211. Heyhat, M.; Kowsary, F.; Rashidi, A.; Esfehani, S.A.V.; Amrollahi, A. Experimental investigation of turbulent flow and convective heat transfer characteristics of alumina water nanofluids in fully developed flow regime. *Int. Commun. Heat Mass Transf.* **2012**, *39*, 1272–1278. [CrossRef]

212. Ahmed, H.E.; Ahmed, M.; Yusoff, M. Heat transfer enhancement in a triangular duct using compound nanofluids and turbulators. *Appl. Therm. Eng.* **2015**, *91*, 191–201. [CrossRef]

213. Koo, J.; Kleinstreuer, C. A new thermal conductivity model for nanofluids. *J. Nanoparticle Res.* **2004**, *6*, 577–588. [CrossRef]

214. Vajjha, R.S.; Das, D.K. Experimental determination of thermal conductivity of three nanofluids and development of new correlations. *Int. J. Heat Mass Transf.* **2009**, *52*, 4675–4682. [CrossRef]

215. Kherbeet, A.; Mohammed, H.A.; Salman, B.; Ahmed, H.; Alawi, O.A.; Rashidi, M.M. Experimental study of nanofluid flow and heat transfer over microscale backward- and forward-facing steps. *Exp. Therm. Fluid Sci.* **2015**, *65*, 13–21. [CrossRef]

216. Vajjha, R.S.; Das, D.K.; Kulkarni, D.P. Development of new correlations for convective heat transfer and friction factor in turbulent regime for nanofluids. *Int. J. Heat Mass Transf.* **2010**, *53*, 4607–4618. [CrossRef]

217. Myers, T.G.; Ribera, H.; Cregan, V. Does mathematics contribute to the nanofluid debate? *Int. J. Heat Mass Transf.* **2017**, *111*, 279–288. [CrossRef]

218. Haddad, Z.; Oztop, H.F.; Abu-Nada, E.; Mataoui, A. A review on natural convective heat transfer of nanofluids. *Renew. Sustain. Energy Rev.* **2012**, *16*, 5363–5378. [CrossRef]

219. Haghighi, E.B.; Utomo, A.T.; Ghanbarpour, M.; Zavareh, A.I.; Nowak, E.; Khodabandeh, R.; Pacek, A.W.; Palm, B. Combined effect of physical properties and convective heat transfer coefficient of nanofluids on their cooling efficiency. *Int. Commun. Heat Mass Transf.* **2015**, *68*, 32–42. [CrossRef]

220. Alkasmoul, F.S. *Characterisation of the Properties and Performance of Nanofluid Coolants with Analysis of Their Feasibility for Datacentre Cooling*; University of Leeds: Leeds, UK, 2015.

221. Alkasmoul, F.S.; Al-Asadi, M.T.; Myers, T.G.; Thompson, H.M. A practical evaluation of the performance of Al_2O_3-water, TiO_2-water and CuO-water nanofluids for convective cooling. *Int. J. Heat Mass Transf.* **2018**, *126*, 639–651. [CrossRef]

222. Xia, G.; Liu, R.; Wang, J.; Du, M. The characteristics of convective heat transfer in microchannel heat sinks using Al_2O_3 and TiO_2 nanofluids. *Int. Commun. Heat Mass Transf.* **2016**, *76*, 256–264. [CrossRef]

223. Hussien, A.A.; Abdullah, M.Z.; Al-Nimr, M.A. Single-phase heat transfer enhancement in micro/minichannels using nanofluids: Theory and applications. *Appl. Energy* **2016**, *164*, 733–755. [CrossRef]

224. Rosa, P.; Karayiannis, T.; Collins, M. Single-phase heat transfer in microchannels: The importance of scaling effects. *Appl. Therm. Eng.* **2009**, *29*, 3447–3468. [CrossRef]

225. Kandlikar, S.G. History, Advances, and Challenges in Liquid Flow and Flow Boiling Heat Transfer in Microchannels: A Critical Review. *J. Heat Transf.* **2012**, *134*, 034001. [CrossRef]

226. Adham, A.P.D.A.M.; Mohd-Ghazali, N.; Ahmad, R. Thermal and hydrodynamic analysis of microchannel heat sinks: A review. *Renew. Sustain. Energy Rev.* **2013**, *21*, 614–622. [CrossRef]

227. Al-Asadi, M.T.; Wilson, M.C.T. Evaluation of nanofluid performance with vortex generators for enhanced micro-channel heat transfer. In Proceedings of the Eleven International Conference on Thermal Engineering: Theory and Applications, Doha, Qatar, 25–28 February 2018.

228. Millan, J.; Godignon, P.; Perpiñà, X.; Perez-Tomas, A.; Rebollo, J. A Survey of Wide Bandgap Power Semiconductor Devices. *IEEE Trans. Power Electron.* **2014**, *29*, 2155–2163. [CrossRef]

229. Al-Asadi, W.T.A.-S. Do ionic liquids replace water or nanofluids to enhance heat transfer in micro-channel systems? In Proceedings of the XI International Conference on Computational Heat and Mass Transfer, Cracow, Poland, 21–24 May 2018.

230. Webb, R. Performance evaluation criteria for use of enhanced heat transfer surfaces in heat exchanger design. *Int. J. Heat Mass Transf.* **1981**, *24*, 715–726. [CrossRef]

231. Zhang, J.; Diao, Y.; Zhao, Y.; Zhang, Y.; Sun, Q. Thermal-hydraulic performance of multiport microchannel flat tube with a sawtooth fin structure. *Int. J. Therm. Sci.* **2014**, *84*, 175–183. [CrossRef]

232. Bushehri, M.R.S.; Ramin, H.; Salimpour, M.R. A new coupling method for slip-flow and conjugate heat transfer in a parallel plate micro heat sink. *Int. J. Therm. Sci.* **2015**, *89*, 174–184. [CrossRef]

233. Nonino, C.; Savino, S.; Del Giudice, S.; Mansutti, L. Conjugate forced convection and heat conduction in circular microchannels. *Int. J. Heat Fluid Flow* **2009**, *30*, 823–830. [CrossRef]

234. Knupp, D.; Cotta, R.; Naveira-Cotta, C.P. Heat Transfer in Microchannels with Upstream–Downstream Regions Coupling and Wall Conjugation Effects. *Numer. Heat Transf. Part B Fundam.* **2013**, *64*, 365–387. [CrossRef]

235. Qu, W.; Mudawar, I. Analysis of three-dimensional heat transfer in micro-channel heat sinks. *Int. J. Heat Mass Transf.* **2002**, *45*, 3973–3985. [CrossRef]

236. Kawano, K.; Minakami, K.; Iwasaki, H.; Ishizuka, M. Micro channel heat exchanger for cooling electrical equipment. *ASME Heat Transf. Div. Publ. Htd.* **1998**, *361*, 173–180.

237. Wu, J.M.; Tao, W.Q. Numerical study on laminar convection heat transfer in a rectangular channel with longitudinal vortex generator. Part A: Verification of field synergy principle. *Int. J. Heat Mass Transf.* **2008**, *51*, 1179–1191. [CrossRef]

238. Safaei, M.R.; Gooarzi, M.; Akbari, O.A.; Shadloo, M.S.; Dahari, M. Performance Evaluation of Nanofluids in an Inclined Ribbed Microchannel for Electronic Cooling Applications. In *Electronics Cooling*; Murshed, S.M.S., Ed.; InTech Open: London, UK, 2016.

239. Habchi, C.; Russeil, S.; Bougeard, D.; Harion, J.-L.; Lemenand, T.; Della Valle, D.; Peerhossaini, H. Enhancing heat transfer in vortex generator-type multifunctional heat exchangers. *Appl. Therm. Eng.* **2012**, *38*, 14–25. [CrossRef]